Crystal Structure and Surface Phase Composition of Palladium Oxides Thin Films for Gas Sensors

A. Samoylov[1], S. Ryabtsev[1], O. Chuvenkova[2], S. Ivkov[1], M. Sharov[1], S. Turishchev[2]

[1]Voronezh State University, Voronezh, Russian Federation

[2]Moscow State University, Moscow, Russian Federation

E-mail: samoylov@chem.vsu.ru

The Contents

In presentation I shall focus on ten major issues:

1. Introduction – The Toxicity of Ozone and NO_2;
2. How Does Gas Sensor Work?;
3. Motivation – Why PdO has been chosen?
4. State of the Art - Our Previous Results;
5. Problem of PdO film Nonstoichiometry;
6. An Improved Experimental Approach;
7. Material Preparation Procedures;
8. Experimental Results;
9. Discussion of the Experimental Results;
10. Summary and Conclusion;
11. Future Works

I

Bec **ısed by atmospheric pollution, air quality control is becoming of great interest in industrialized countries.**

Introduction

WHO and **US EPA** have established that ***three*** out of ***six common air pollutants*** (also called as "**criteria pollutants**") are the oxidizing gases: ***sulfur dioxide***, ***nitrogen oxides***, and ***low level ozone*** (or ***tropospheric ozone***).

Introduction
«Good» and «Bad» Ozone

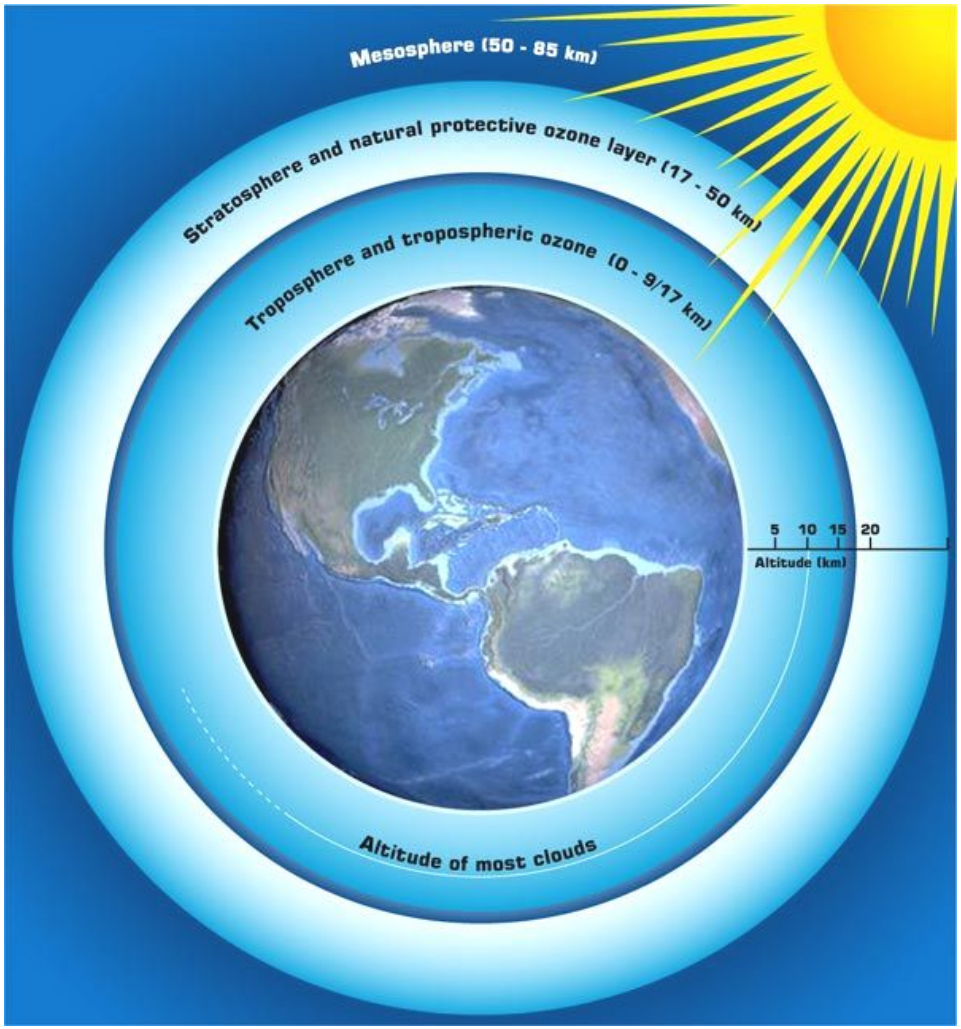

It is well known the expression that *ozone gas is like a double edged sword*. Most of the atmospheric ozone (90%) is located in the stratosphere with a maximum concentration between 17 and 25 km. Without ozone in the atmosphere, it would be too dangerous to walk outside without having to wear some sort of special suit.

Introduction

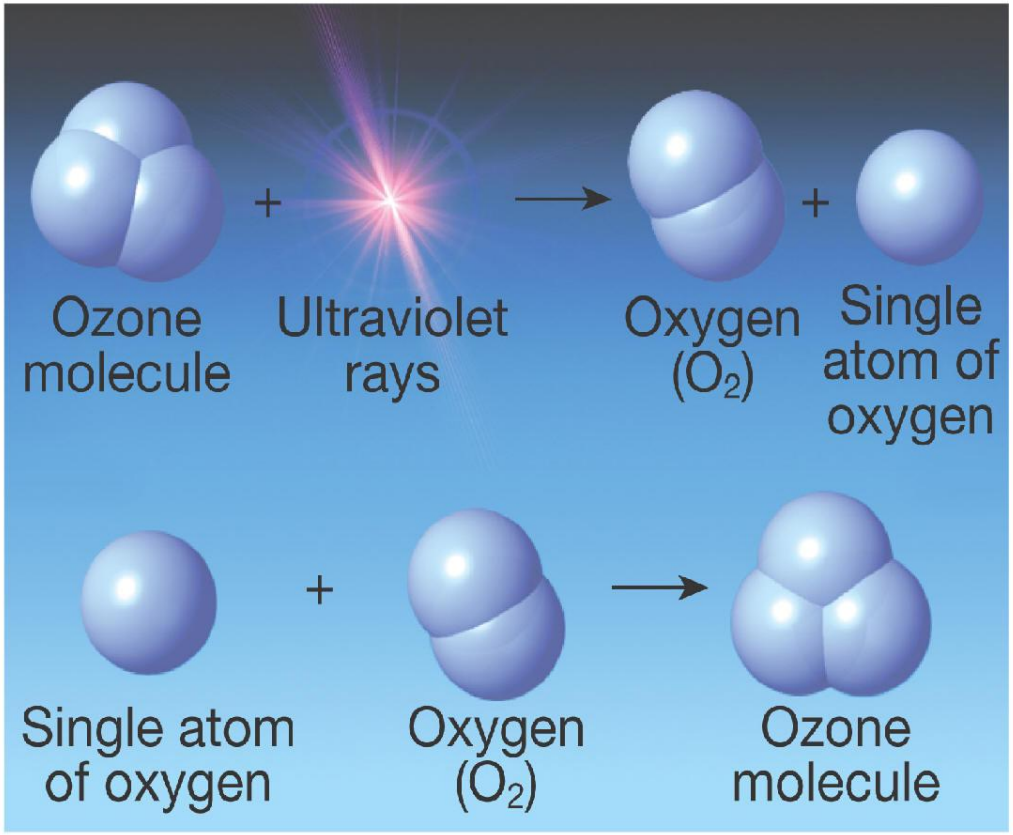

The chemical reactions of ozone O_3 and oxygen O_2 under influence of UV rays.

When ozone is concentrated in the lower stratosphere, it actually protects people, animals, and plants from the sun's harmful UV rays.

Introduction

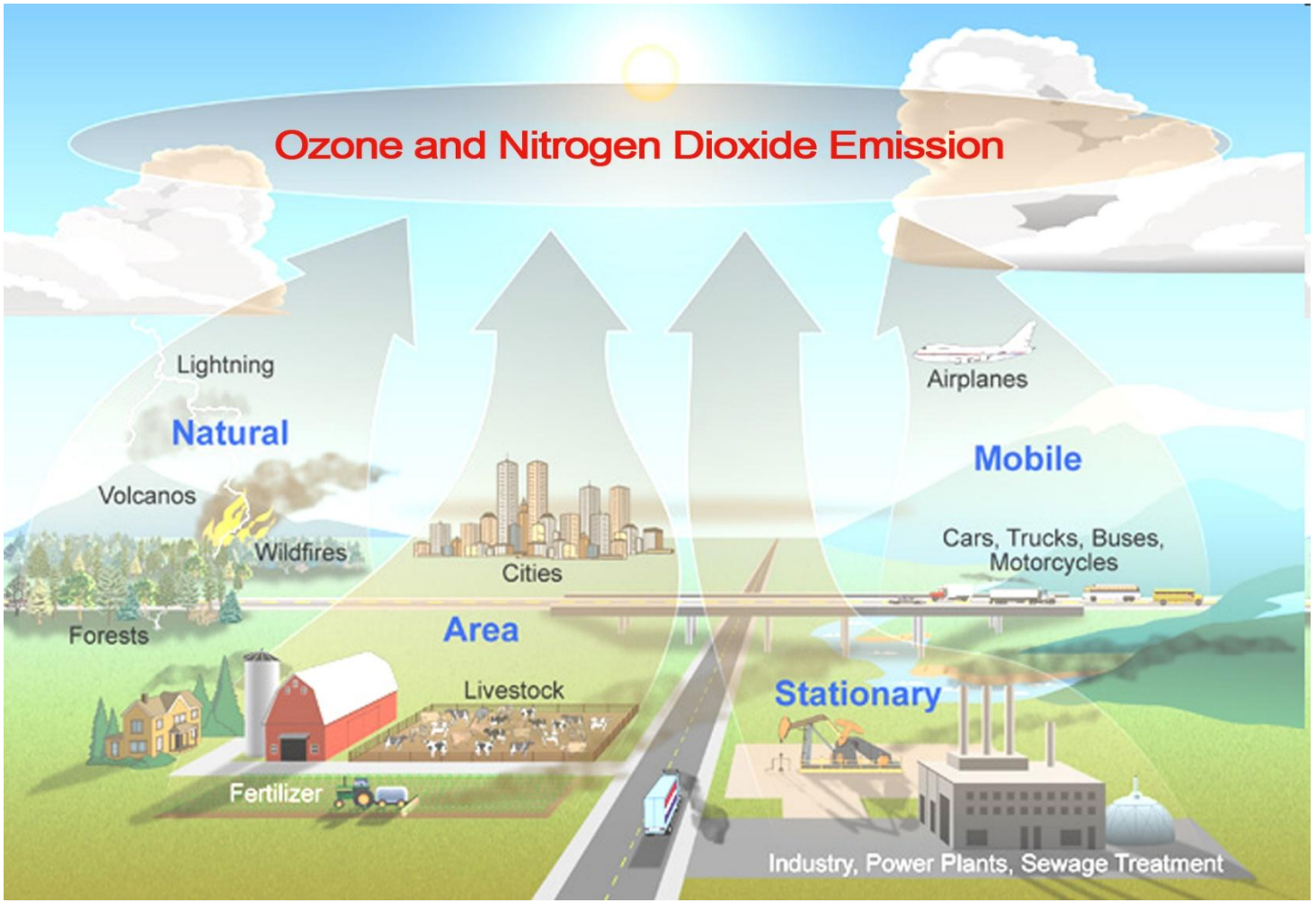

The main sources of ozone and nitrogen oxides ambient air pollution.

Introduction

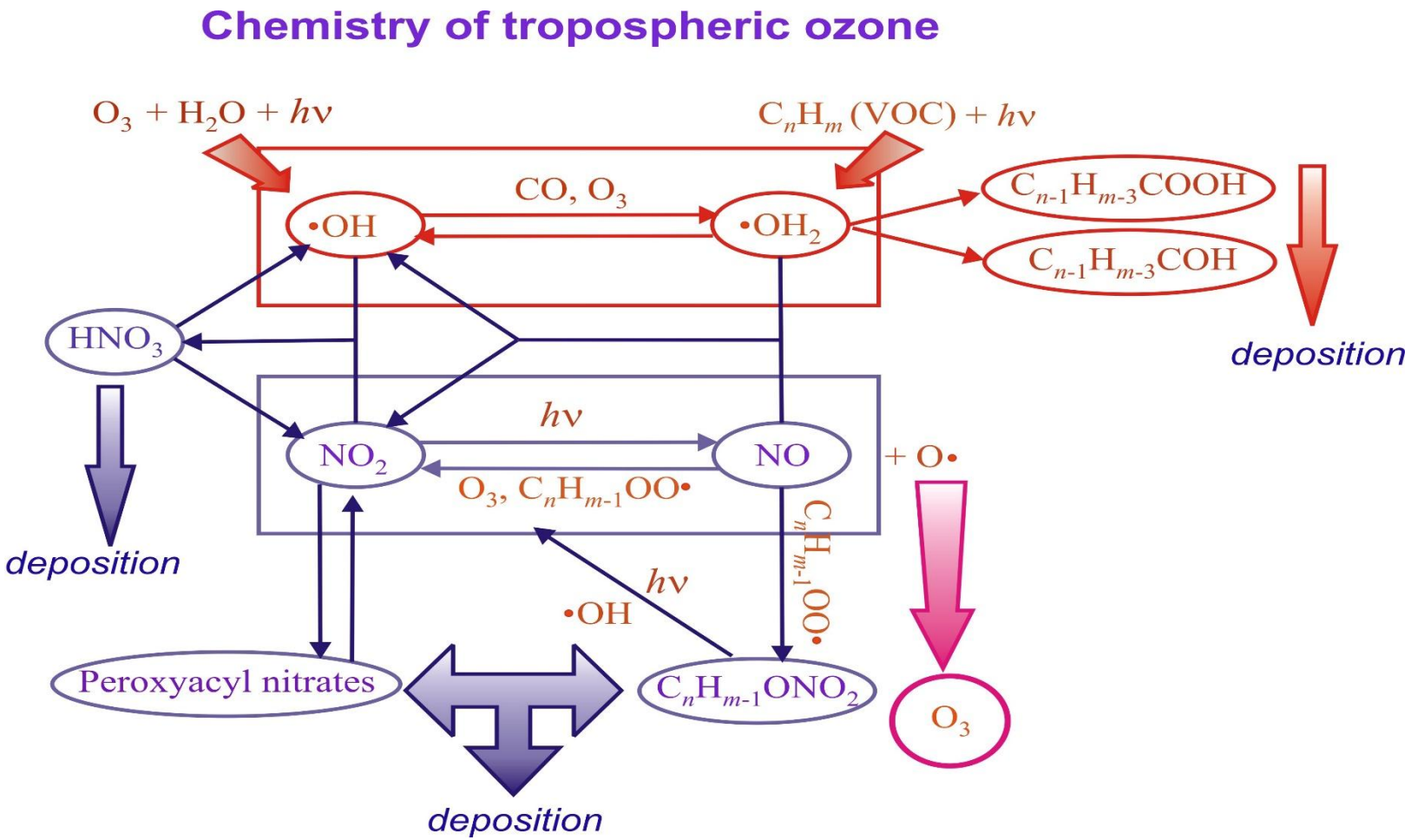

The chemical reactions of tropospheric ozone and nitrogen dioxide under sunlight.

Introduction

- A Nasal cavity
- B Pharynx
- C Larynx
- D Trachea
- E Alveoli
- F Bronchial tree
- G Diaphragm

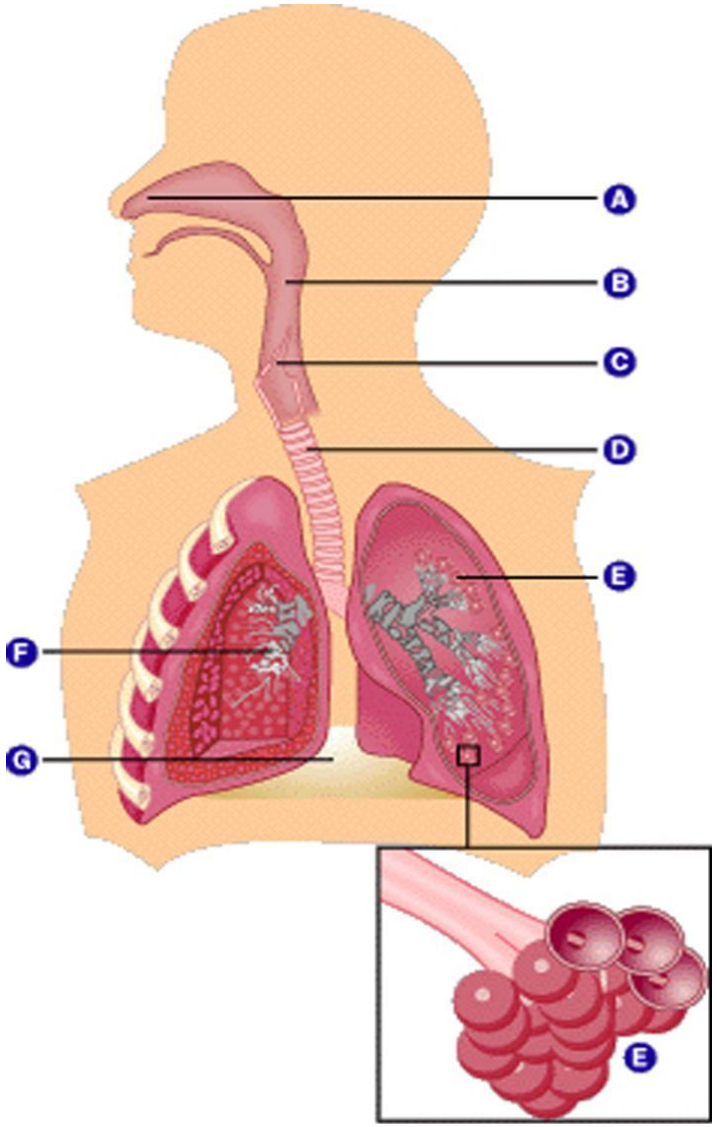

Breathing ozone and nitrogen oxides can trigger a variety of human health problems, particularly for children, the elderly, and people who have lung diseases.

Introduction

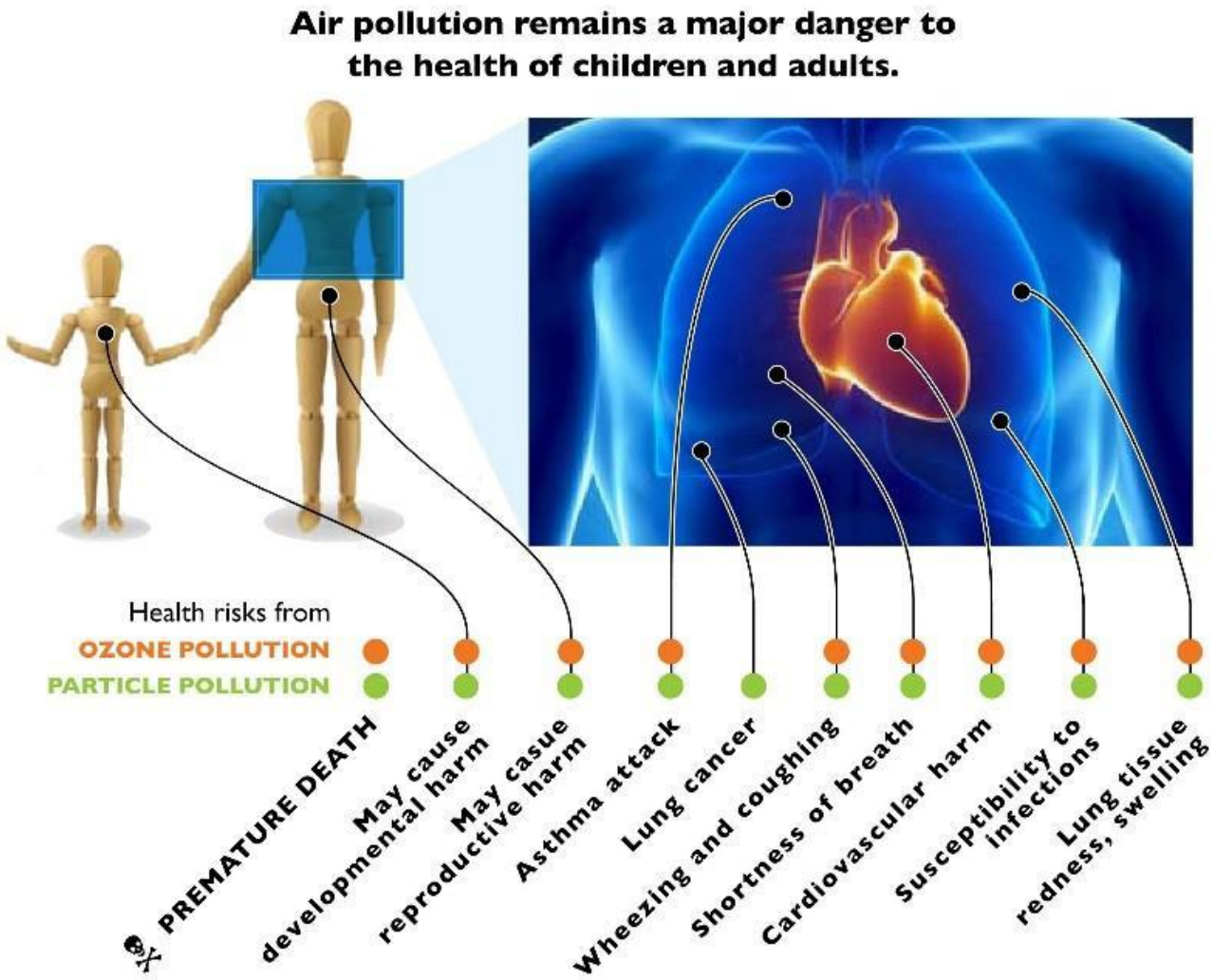

Introduction

The plant upon the ozone influence (left) and this plant in normal air conditions (right).

!!! Ozone is more toxic than phosgene – the chemical weapon !!!

The values of maximum permissible concentration (critical concentration) averaged over one hour of ozone and nitrogen dioxide in industrialized countries.

Country / Gas	USA	UK	Japan	EC
Ozone	70 – 75 ppb	200 ppb	100 ppb	105 ppb
Nitrogen dioxide	100 ppb	100 ppb	100 ppb	100 ppb

Introduction

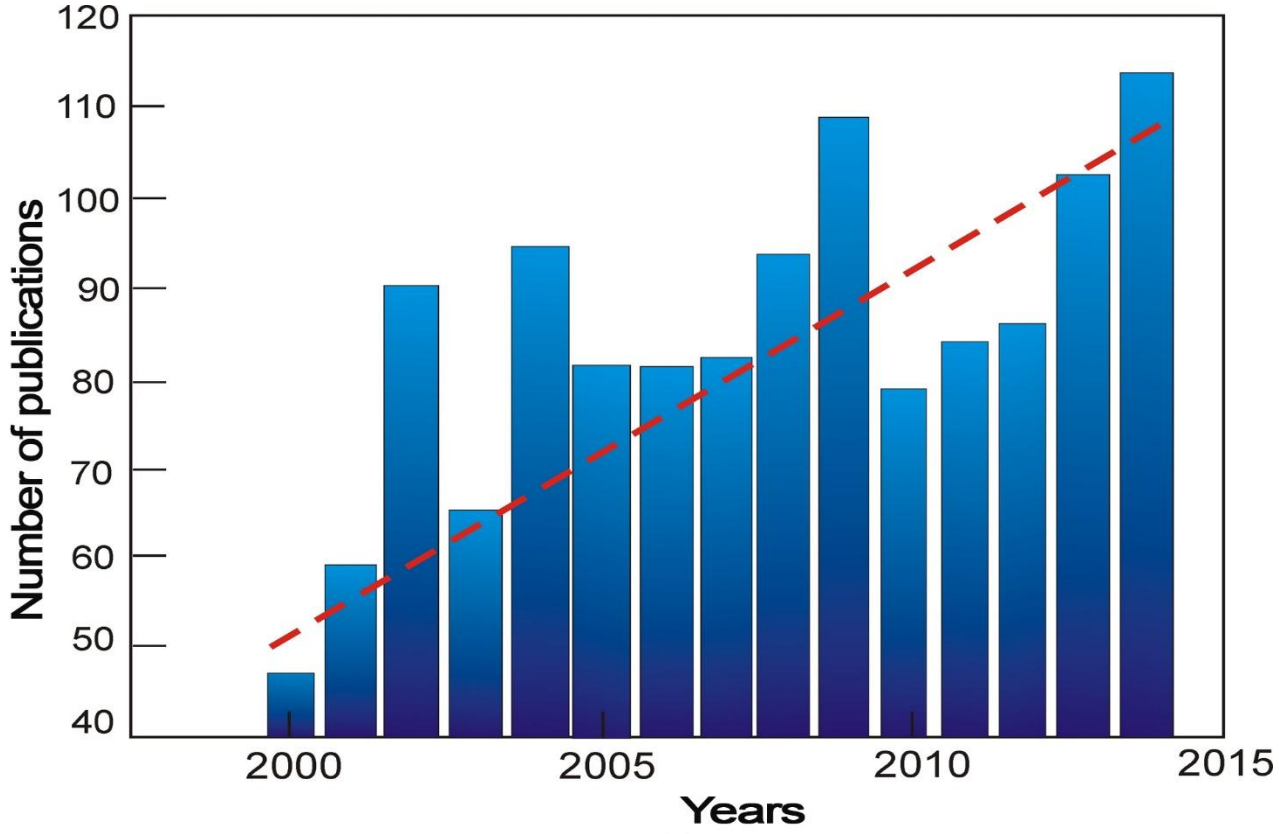

The growth in the number of publications devoted to the design of ozone sensors. Data extracted from Scopus and Web of Science [1].

[1]. Korotcenkov G., Brinzari V., Cho B.K. In_2O_3- and SnO_2-Based Thin Film Ozone Sensors: Fundamentals // Journal of Sensors. − 2016. − V. 2016, Article ID 3816094. − P. 1−31.

How does metal oxide gas sensor work?

***n*-type metal oxide semiconductor gas sensor**

***p*-type metal oxide semiconductor gas sensor**

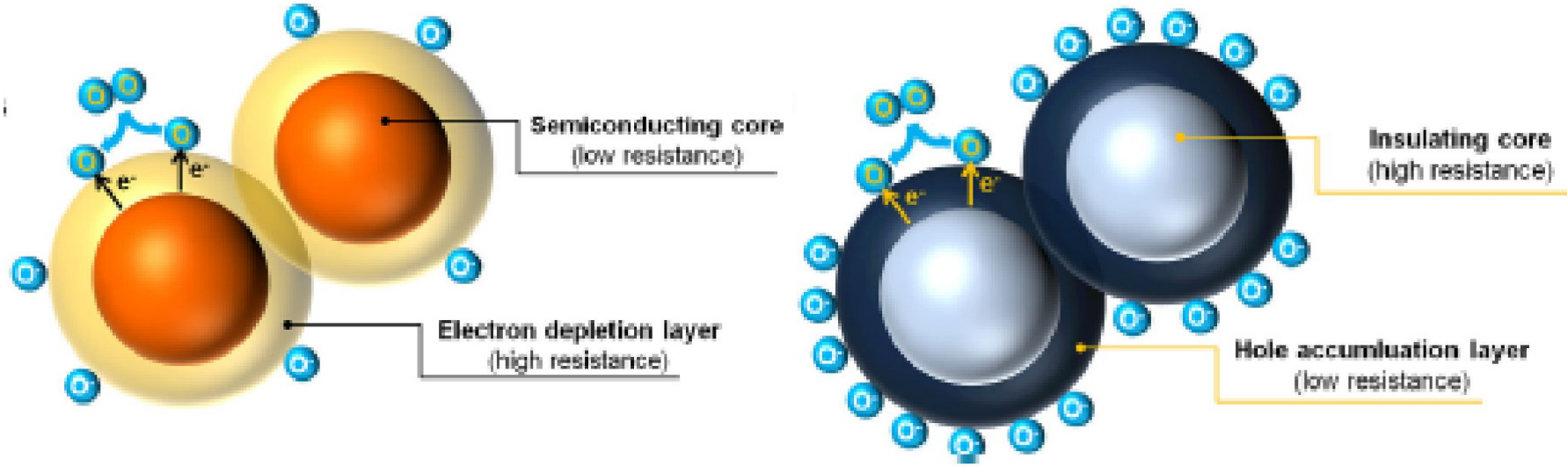

Formation of electronic core–shell structures in (a) *n*-type and (b) *p*-type oxide semiconductors.

[2]. Hyo-Joong Kim, Jong-Heun Lee. Highly sensitive and selective gas sensors using *p*-type oxide semiconductors: Overview // **Sensors and Actuators B**. 2014, V. 192. P. 607– 627.

How does metal oxide gas sensor work?

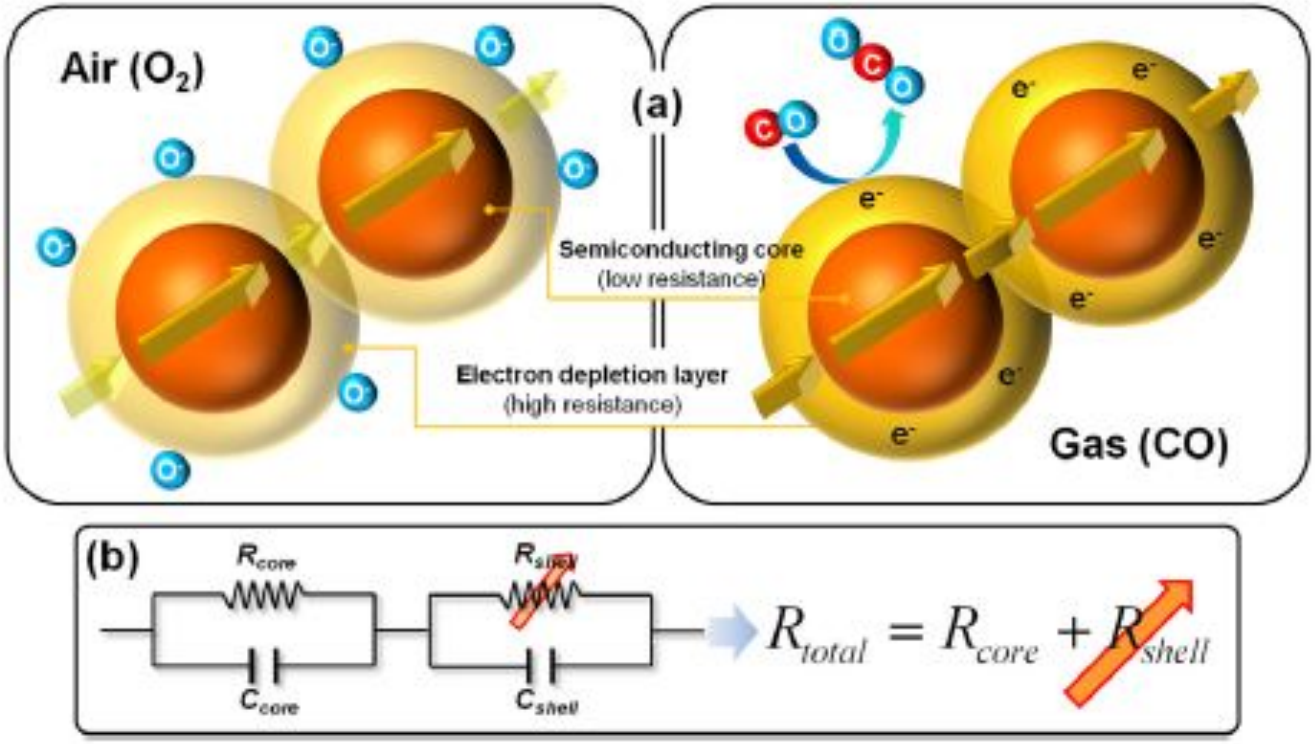

a)

b)

Sensing mechanism (*a*) and equivalent electrical circuit (*b*) of *n*-type metal oxide semiconductor during detection of gas with *reductive properties* - carbon monoxide CO.

How does metal oxide gas sensor work?

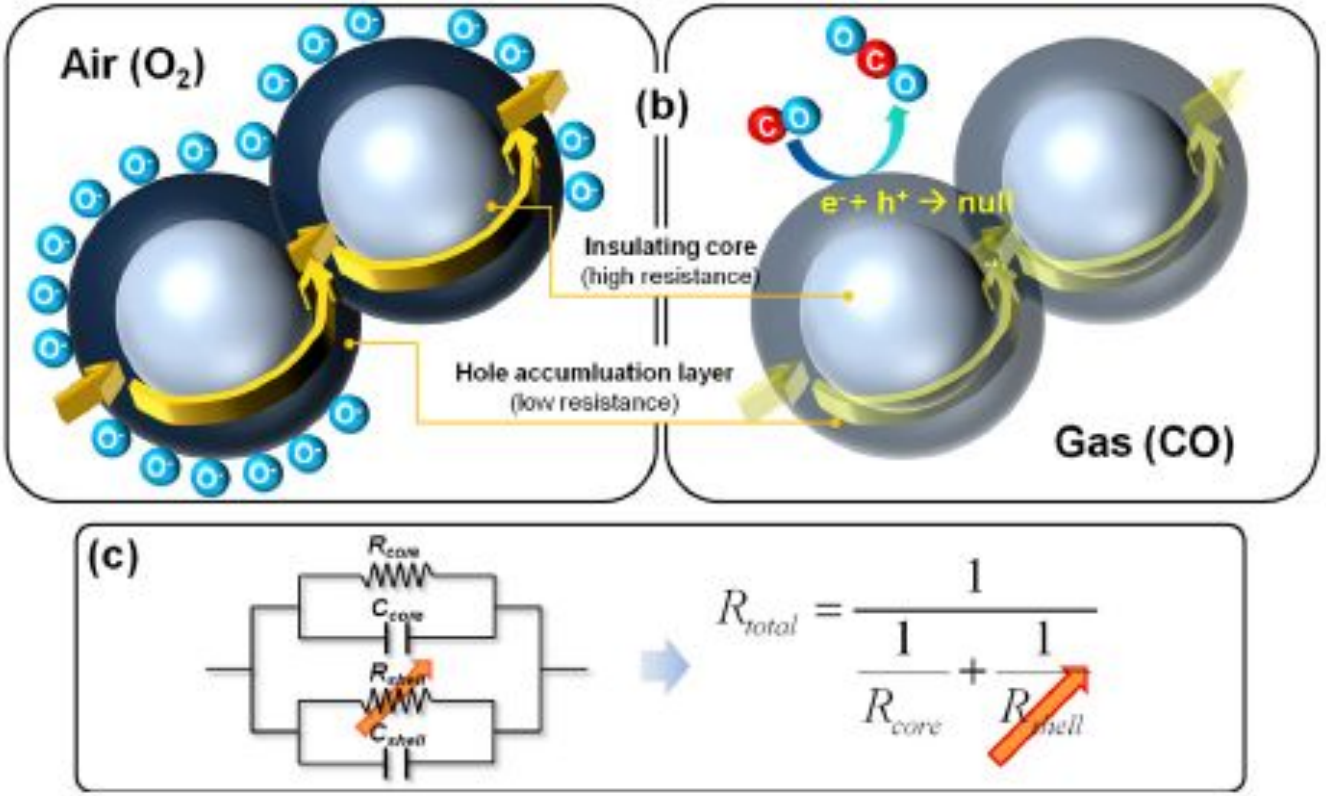

Sensing mechanism (*a*) and equivalent electrical circuit (*b*) of *p*-type metal oxide semiconductor during detection of gas with *reductive properties* - carbon monoxide CO.

Motivation - Why PdO has been chosen?

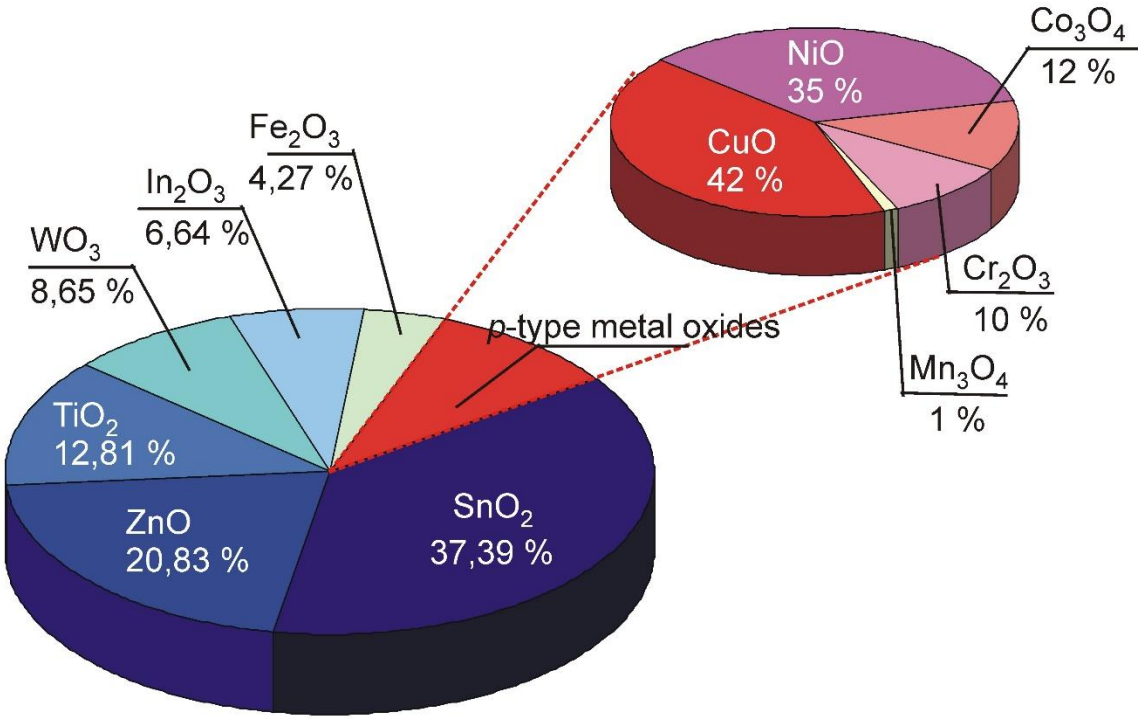

Studies on *n*- and *p*-type oxide semiconductor gas sensors [2].

!!! There is not Palladium Oxide in the list of p-type Metal Oxides for Gas Sensors !!!

[2]. Hyo-Joong Kim, Jong-Heun Lee. Highly sensitive and selective gas sensors using *p*-type oxide semiconductors: Overview // **Sensors and Actuators B. 2014**, V. 192. P. 607– 627.

Motivation - Why PdO has been chosen?

In the end of 2015 for the first time our research group presented thin and ultra thin films of palladium (II) oxide as new promising material for toxic oxidizing gas detection.

The choice of palladium (II) oxide as the material for gas sensors was not incidental. It was done because of *some reasons*:

1. Long recovery process and high stability could be referred to the main disadvantages of the SnO_2-based oxidizing gas sensors;

2. Late transition metals, such as Pd, Pt and Au, have been widely used as additives to improve gas-sensing performance of tin dioxide;

3. There is an opinion that the metal oxides semiconductors with *p*-type conductivity are more promising than materials with *n*-type conductivity for oxidizing gas detection.

State of the Art – our Previous Results

Fabrication of initial Pd films (d = 10 – 35 nm) :
– thermal sublimation of palladium foil (purity was 99.99 per cent) in high vacuum and condensation of metal vapours on different substrates;

Temperature dependence of Pd vapour pressure over solid Pd foil:

$$\log_{10} P(\mathrm{Pd}^{s},\ \mathrm{Pa}) = -\frac{20150}{T} + 13.670 - 0.419\log_{10} T - 0.302\times 10^{-3} T$$

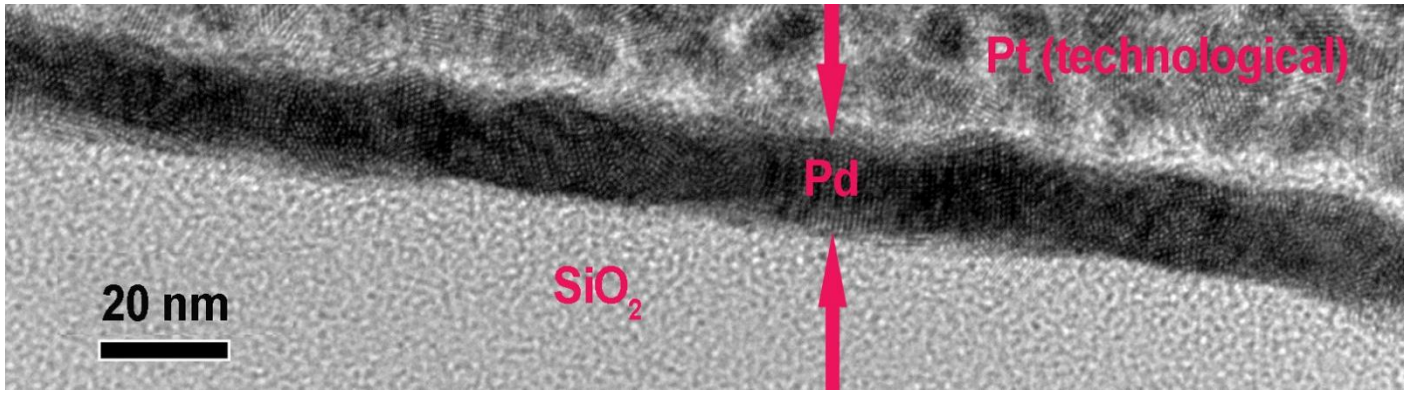

The bright field (BF) HR TEM image of x cross section of Pd/SiO_2/Si (100) heterostructures (samples were prepared by FIB technique).

State of the Art - our Previous Results

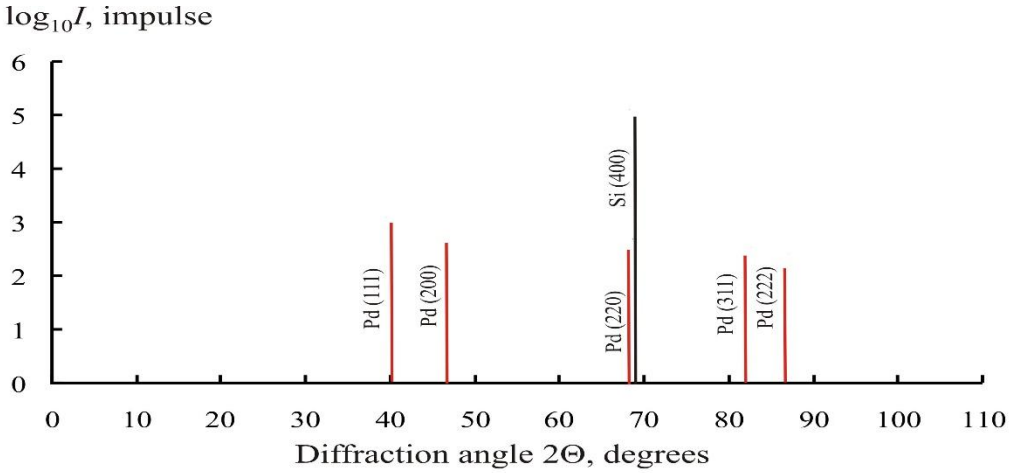

1)

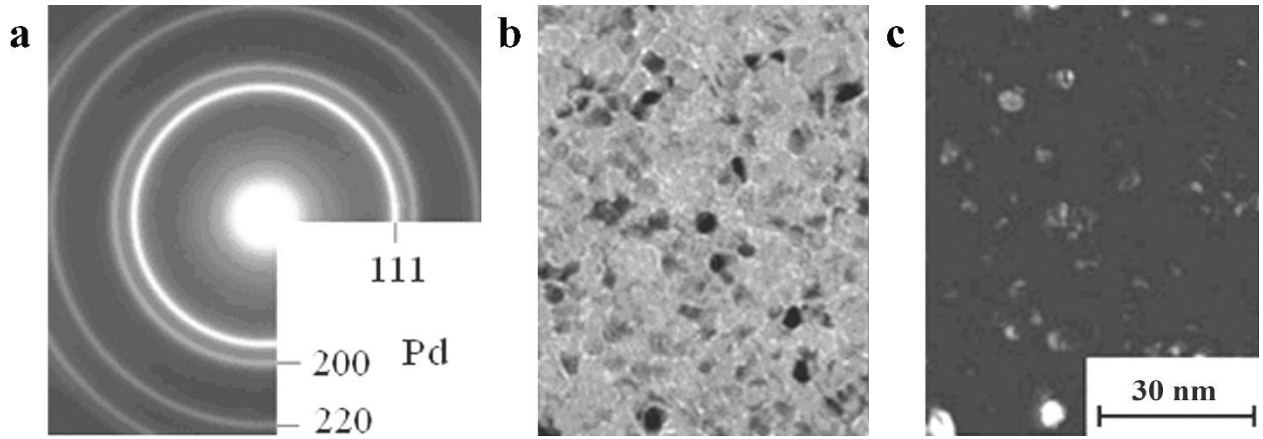

2)

XRD (*1*) and THEED patterns (*2* a) of initial Pd film (*d* = 35 nm) on Si (100) substrate; b) bright-field TEM image, c) dark-field image.

State of the Art - our Previous Results

T_{ox} = 570 K; heterogeneous mixture of Pd and PdO

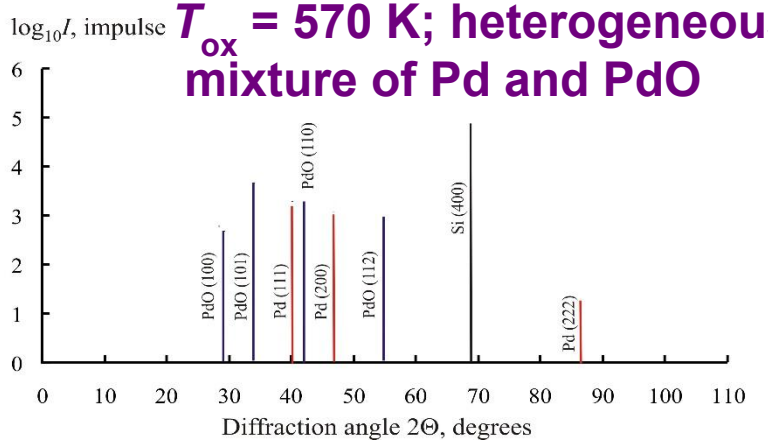

T_{ox} = 770 K; homogeneous, PdO phase only

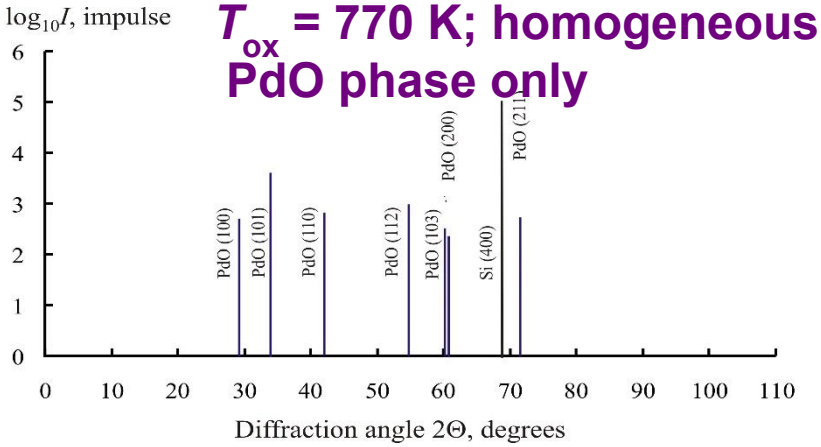

T_{ox} = 870 K; homogeneous, PdO phase only

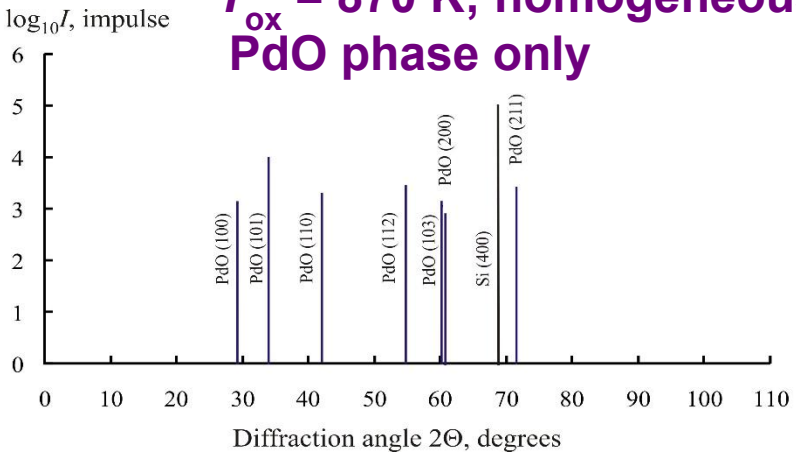

T_{ox} = 1070 K; heterogeneous mixture of PdO and undetermined phase, Pd – Si

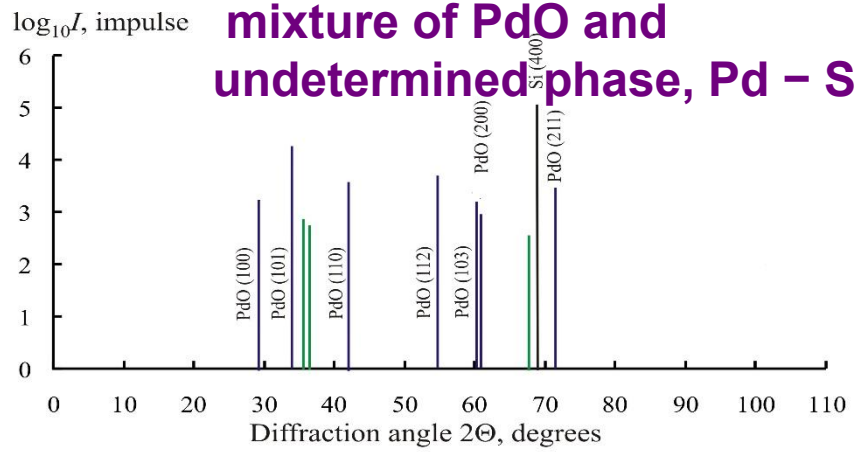

X-ray diffraction patterns of palladium film deposited on Si (100) substrate after oxidation in dry O_2 at T_{ox} = 570 – 1070 K.

State of the Art -Our Previous Results

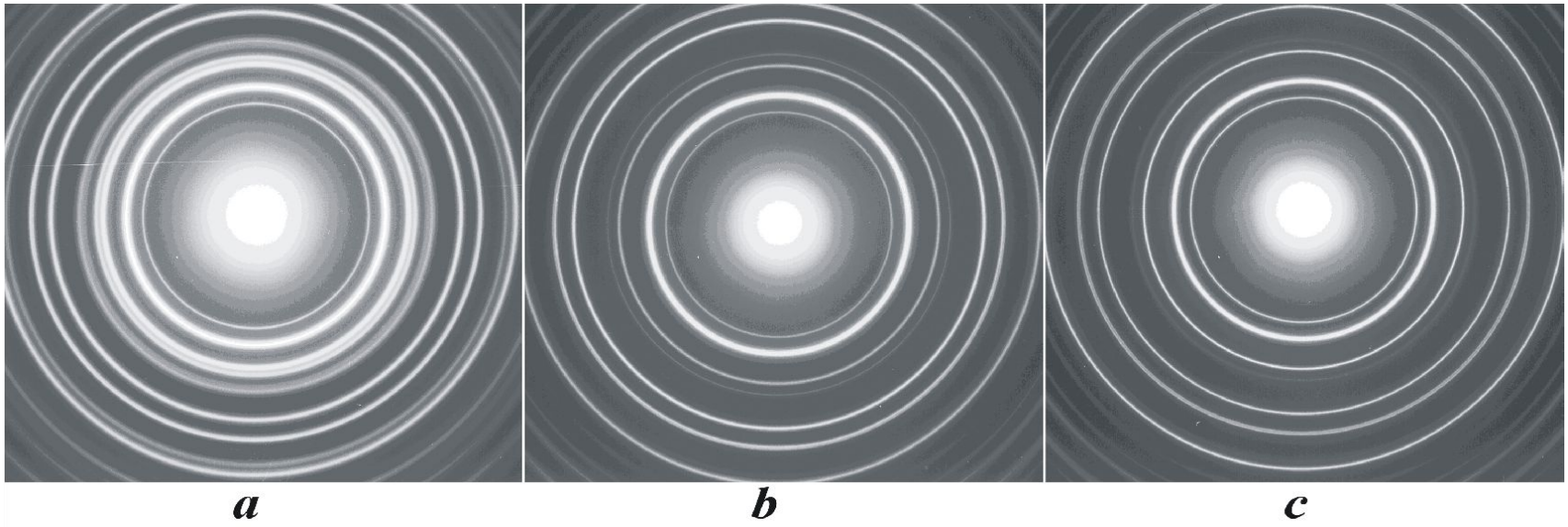

Evolution of Pd thin films HEED patterns after annealing in dry O_2 at different oxidation temperature: *a*) T_{ox} = 573 K (**heterogeneous mixture of Pd and PdO**); *b*) T_{ox} = 773 K (**homogeneous PdO phase);** *c*) T_{ox} = 873 K (**homogeneous PdO** - SG - $P4_2/mmc$) [3].

[3] Ryabtsev S.V., Ievlev V.M., **Samoylov A.M.,** Kuschev S.B., Soldatenko S.A. Microstructure and electrical properties of palladium oxide thin films for oxidizing gases detection // **Thin Solid Films**. – **2017**. – V. 636. – P. 751-759.

State of the Art - Our Previous Results

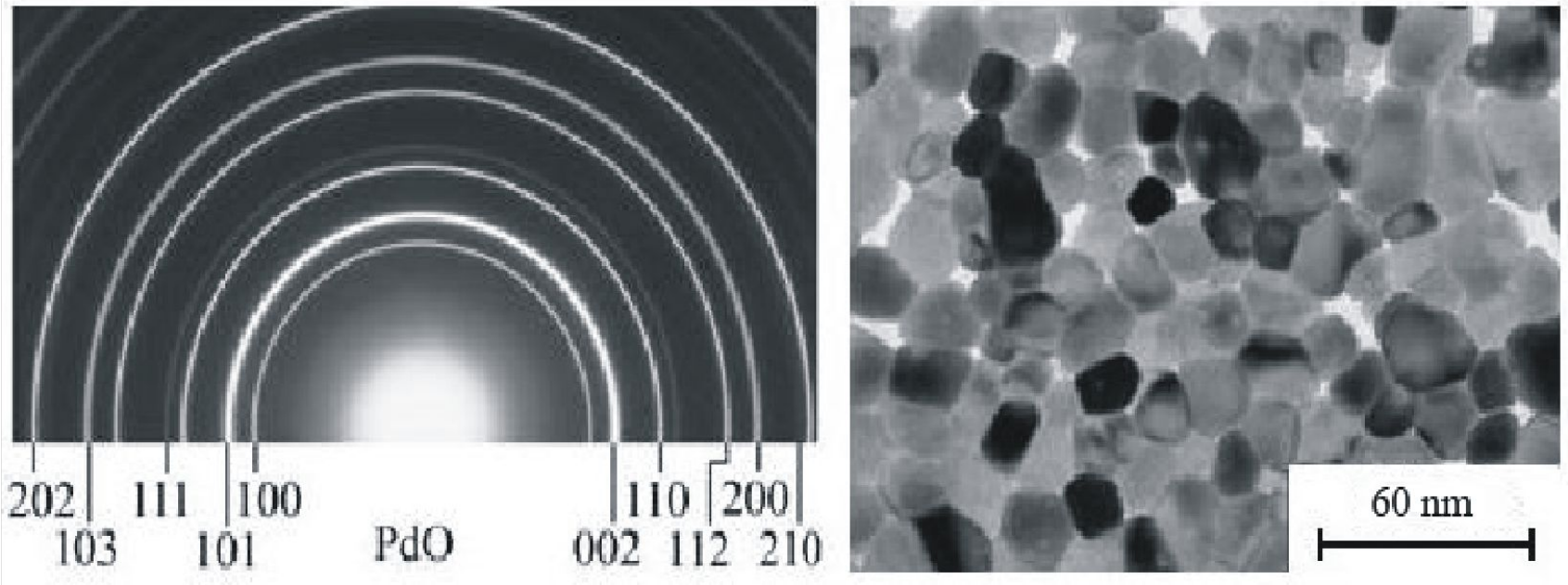

HEED patterns (a) and bright-field TEM image (b) of PdO film prepared by oxidizing procedure at T = 870 K.

State of the Art - Our Previous Results

p-type conductivity of PdO thin films

$$E_{emf} = -S \nabla T,$$

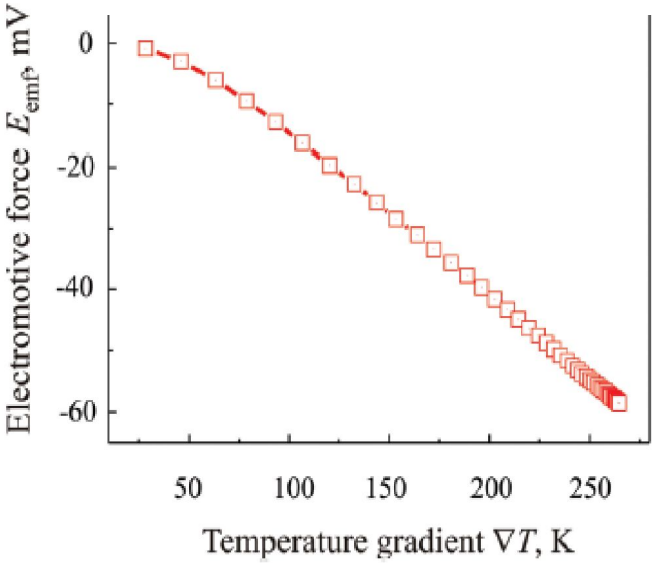

Table 1.

Results of Hall effect measurements for PdO films prepared by oxidation at T_{an} = 870 K and T_{an} = 1070 K (thickness d ~ 35 nm).

PdO film oxidized at T_{an} = 870 K				
Direct current I_x, A	Magnetic field B_z, T	Average Hall voltage $\bar{U}_H$, V	Average Hall coefficient $\bar{R}_H$, m^3/C	Charge carrier density $[p]$, m^{-3}
1×10^{-5}	1.5	0.168	2.84×10^{-4}	~ 2.21×10^{22}
2×10^{-5}	1.5	0.384	3.21×10^{-4}	~ 1.95×10^{22}

Seebeck coefficient *S* = + 120 – +220 μV/K

Temperature dependence of electromotive force E_{emf} (*a*) and results of Hall measurement (*b*) of PdO films prepared by oxidation at T_{ox} = 870 K.

State of the Art - Our Previous Results

Energy band gap of PdO thin films (thickness ~ 35 nm) ΔE_g = 2.3 eV

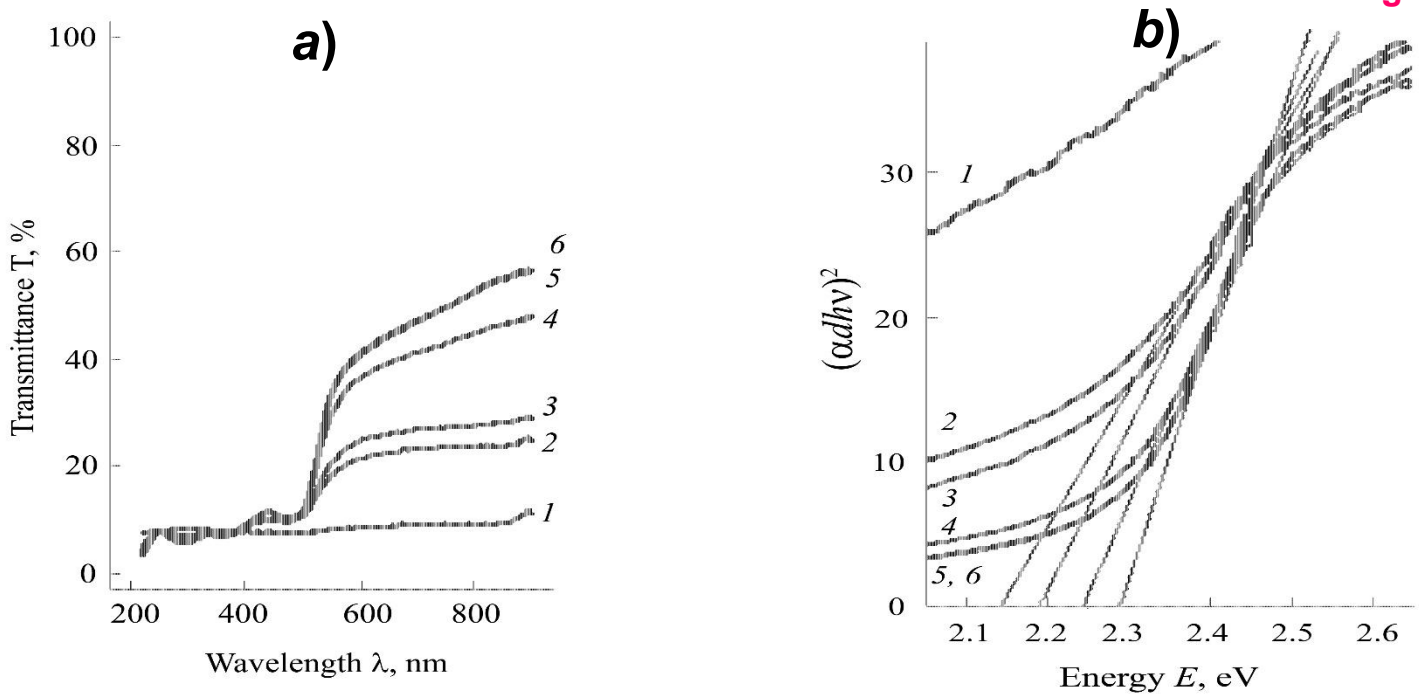

Transmission spectrum of Pd films after oxidizing at different temperatures (***a***) and dependence of $(\alpha dh\nu)^2$ value from photon energy for Pd films oxidizing at dry oxygen at different temperature: *1* - *T* = 510 K; *2* - *T* = 570 K; *3* - *T* = 670 K; *4* - *T* = 770 K; *5* - *T* = 870 K; *6* - *T* = 1070 K [4].

[4] Ryabtsev S.V., **Samoylov A.M.,** Sinelnikov A.A., Ievlev V.M., Shaposhnik A.V., Soldatenko S.A., Kuschev S.B. Thin Films of Palladium Oxide for Gas Sensors // **Doklady Physical Chemistry**. **2016**. V. 470. № 2. P. 158-161.

State of the Art - Our Previous Results

Gas sensor properties of PdO thin films (thickness ~ 35 nm)

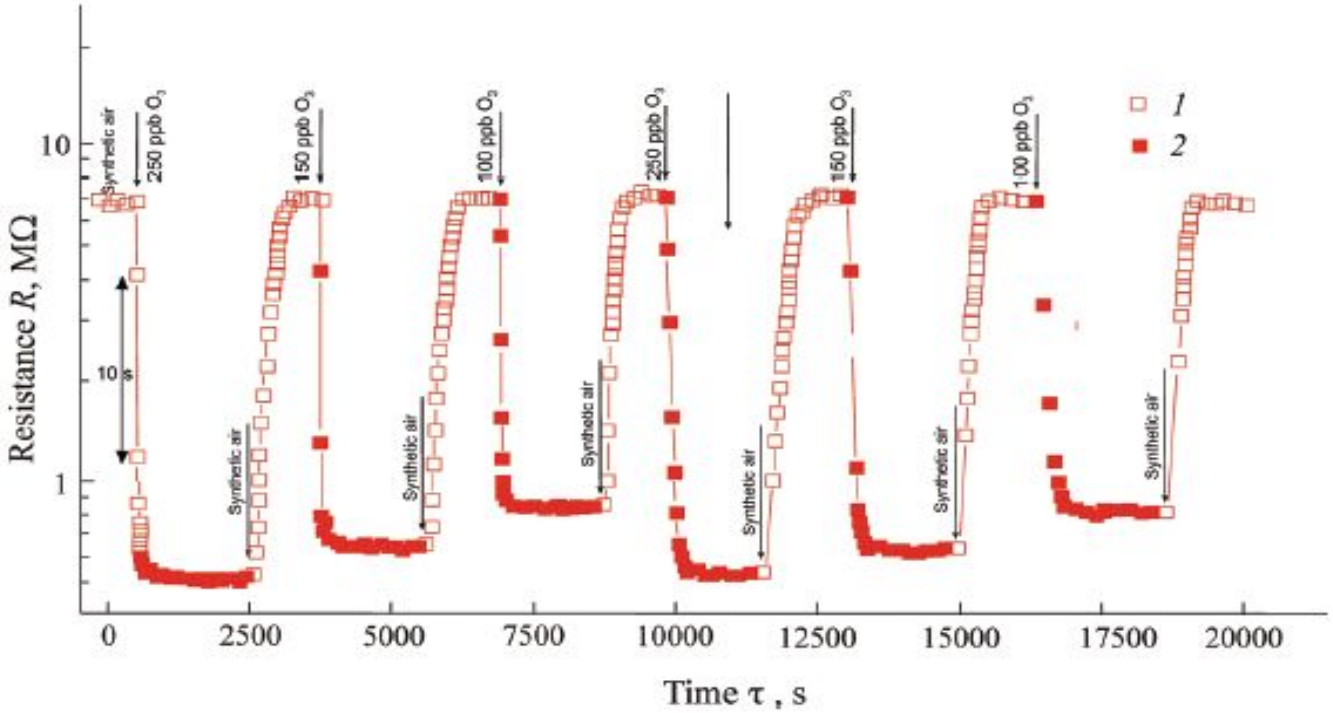

Time dependence of PdO thin film (thickness ~ 35 nm) sensor resistance *R* at ozone different concentrations in SA: prepared by oxidation at T_{ox} = 870 K; operation temperature T_d = 490 K [5].

[5]. **Samoylov A.M.,** Ryabtsev S.V., Popov V.N., Badica P. Palladium (II) Oxide Nanostructures as Promising Materials for Gas Sensors. **In book: Novel Nanomaterials Synthesis and Applications // Edited by George Kyzas. UK, London : IntechOpen Publishing House, 2018**. – P. 211 – 229.

State of the Art - Our Previous Results

Gas sensor properties of PdO ultra thin films (thickness ~ 10 nm)

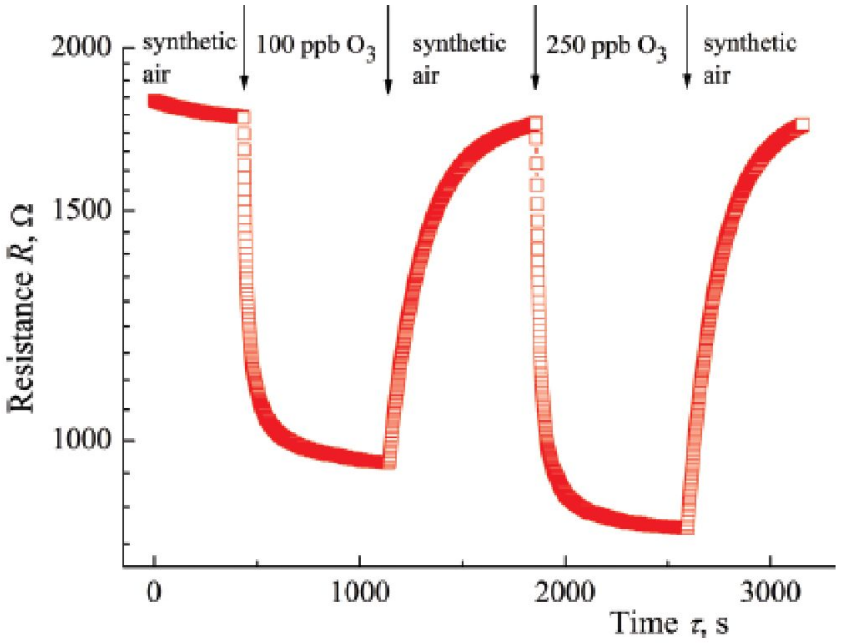

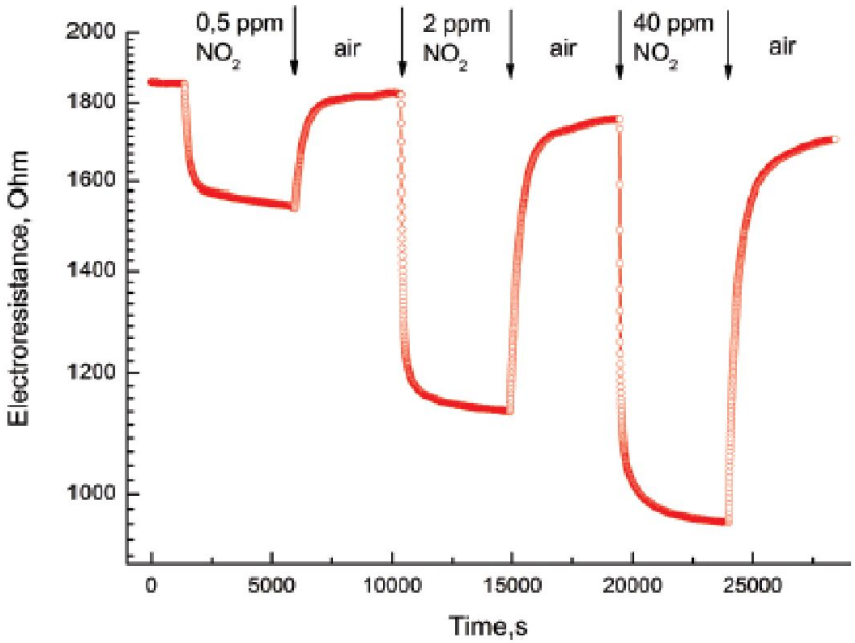

Resistance time dependence of PdO ultra thin films (d ~ 10 nm) at detection of ozone (a) and nitrogen dioxide (b) in SA atmosphere (operation temperature T_d = 450 K) [6].

[6] Ievlev V.M., Ryabtsev S.V., **Samoylov A.M.,** Shaposhnik A.V., Kuschev S.B., Sinelnikov A.A. Thin and Ultrathin Films of Palladium Oxide for Oxidizing Gases Detection. **Sensors and Actuators B: Chemical. – 2018**. – V. 255, N. 2. P. 1335 – 1342.

State of the Art - Our Previous Results

Gas sensor properties of PdO thin films (thickness ~ 35 nm)

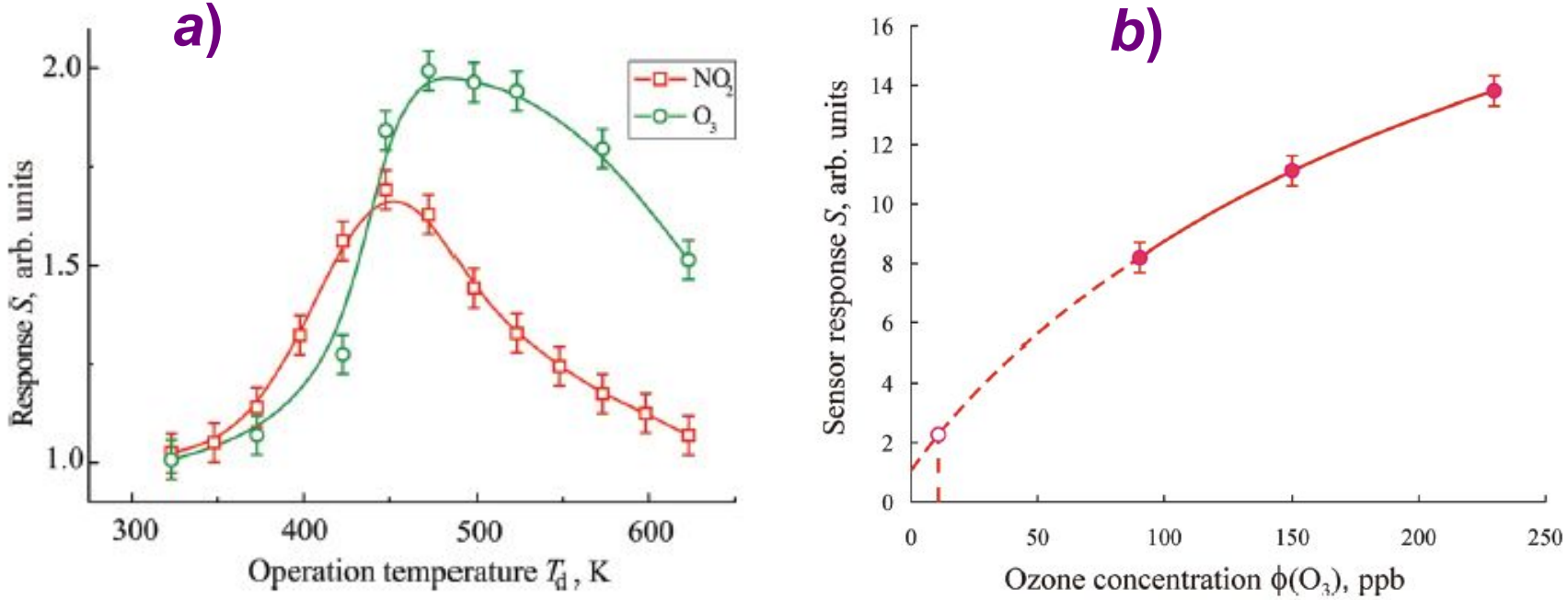

Dependence of sensor response *S* of PdO thin films upon operating temperature T_d (*a*) and analyte gas concentration at detection of ozone and nitrogen dioxide (*b*) [6].

[6] Ievlev V.M., Ryabtsev S.V., **Samoylov A.M.,** Shaposhnik A.V., Kuschev S.B., Sinelnikov A.A. Thin and Ultrathin Films of Palladium Oxide for Oxidizing Gases Detection. **Sensors and Actuators B: Chemical. – 2018.** – V. 255, N. 2. P. 1335 – 1342.

Crystal Structure of PdO

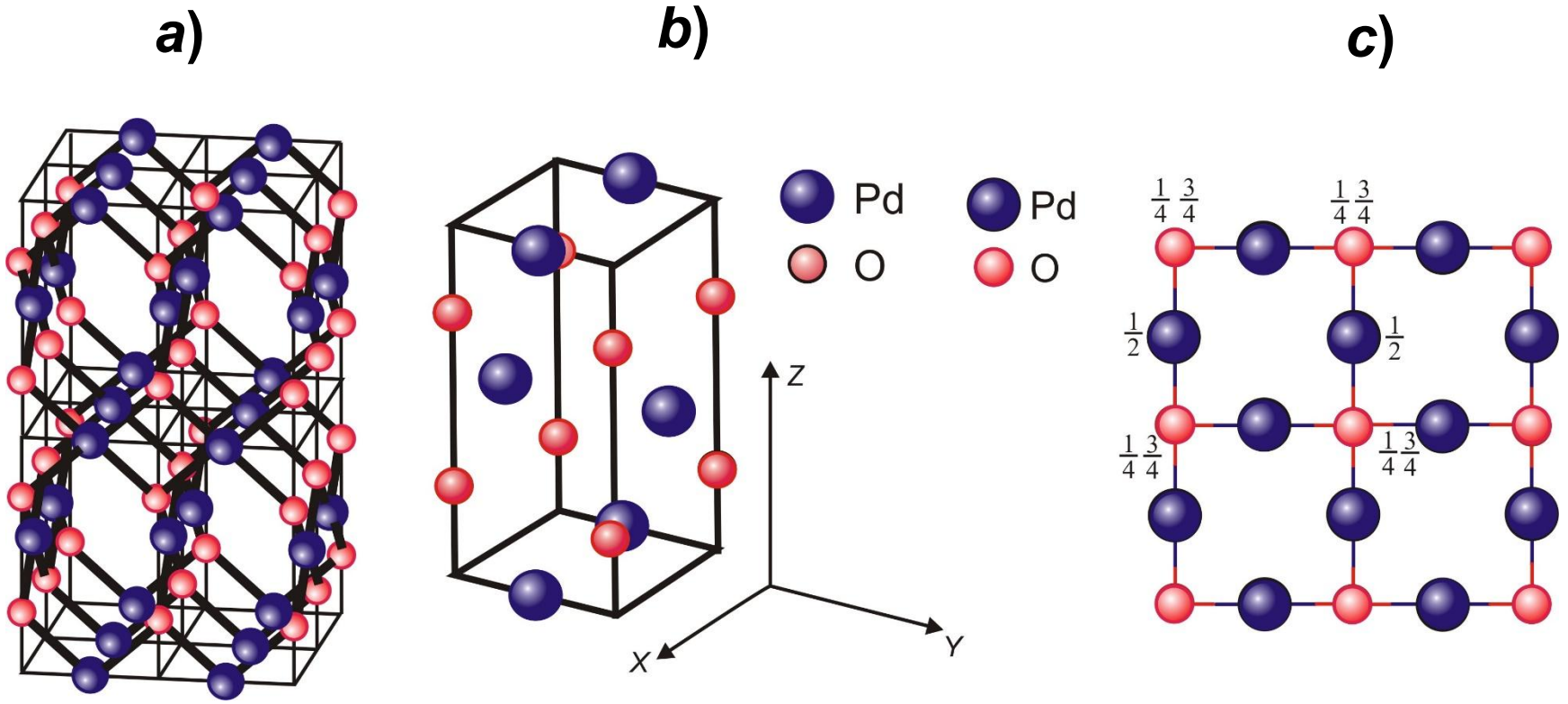

(*a*) Crystal structure of PdO; (*b*) unit cell of PdO tetragonal structure (S.G. $P4_2/mmc$); (*c*) projection of 4 PdO unit cell atoms onto (001) plane – *XOY* plane.

Problem of PdO film Nonstoichiometry

Taking into account the nonstoichiometry of PdO caused by O atom excess, the hole conductivity of PdO films can be explained by two reasons.

1. The existence of Pd vacancies:

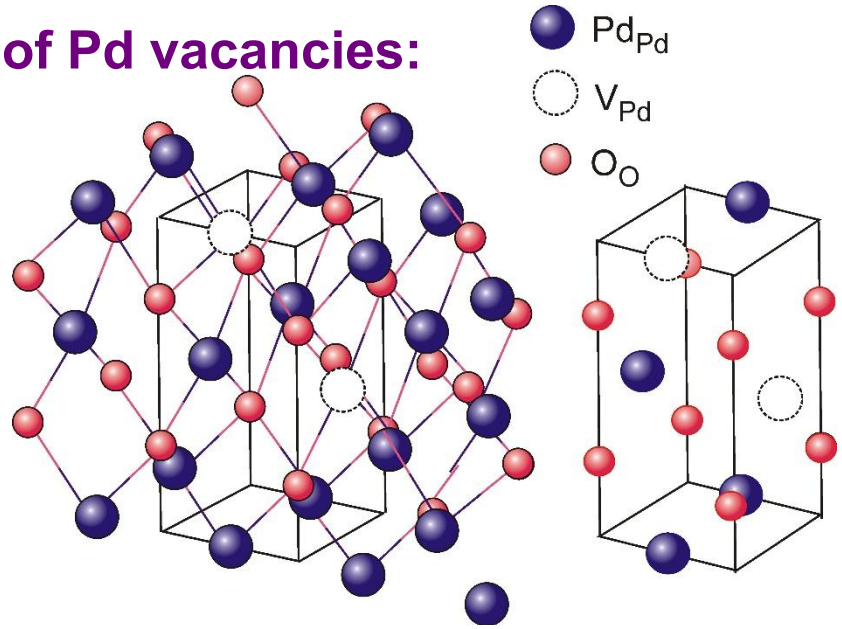

$$Pd^{(S)} + O_2{}^{(G)} \rightarrow Pd_{Pd} + 2O_O + V_{Pd}^{\times}$$

Neutral Pd vacancies are ionized with the hole formation:

$$V_{Pd}^{\times} \rightleftarrows V_{Pd}' + h^{\bullet} \quad \text{or} \quad V_{Pd}^{\times} \rightleftarrows V_{Pd}'' + 2h^{\bullet}$$

Problem of PdO film Nonstoichiometry

2. The existence of oxygen atoms in interstitials:

$$Pd^{(S)} + O_2^{(G)} \rightarrow Pd_{Pd} + O_O + O_i^{\times}$$

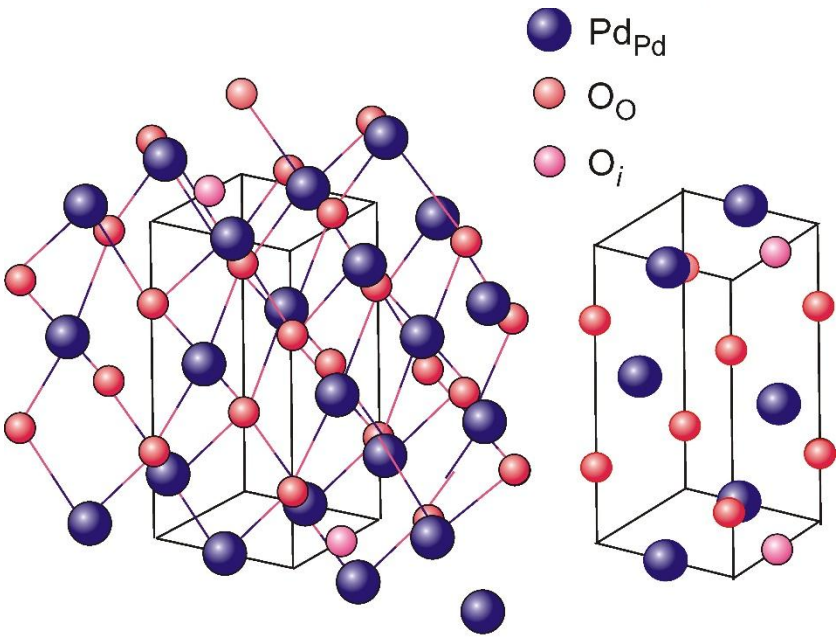

Neutral O atoms in interstitials are ionized with the hole formation

$$O_i^{\times} \rightleftarrows O_i' + h^{\bullet} \quad \text{or} \quad O_i^{\times} \rightleftarrows O_i'' + 2h^{\bullet}$$

The Main Purpose of this Study

The main purpose of this work is the complex study of the evolution of surface phase chemical composition and crystal structure of palladium oxides upon oxidation temperature in dry oxygen.

An Improved Experimental Approach

Previous X-ray study

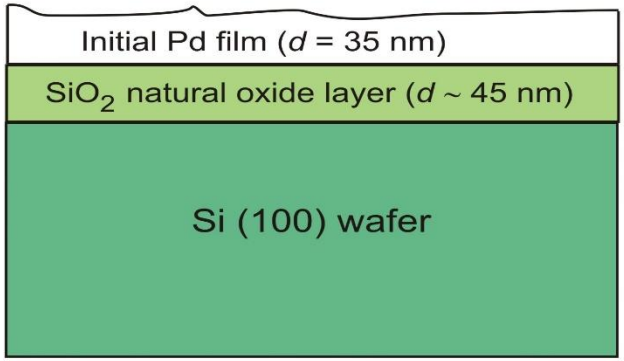

Oxidation in dry O_2, T_{ox} = 1070 K

X-ray study results: Reflexes of PdO + three week peaks of undetermined phase, probably, Pd - Si

Present X-ray study

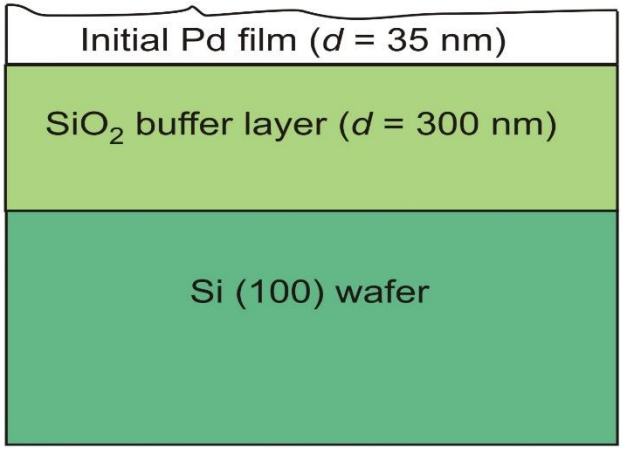

Oxidation in dry O_2, T_{ox} = 1070 K

X-ray study results: Reflexes of PdO only

The Experimental Procedures

1. Thermal sublimation in high vacuum;
2. X-ray diffraction – diffractometer DRON – 8;
3. SEM - JEOL JCM 6880 L;
4. EDS - JEOL JCM 6880 L + Oxford Instruments INCAS sigh
5. TEM – Karl Zeiss Libra 120;
6. Synchrotron radiation of Helmholtz Centrum Berlin (Berlin, Germany) BESSY II storage ring;
7. HR SEM and HR TEM – FEI Titan 80 – 300.

Experimental procedure

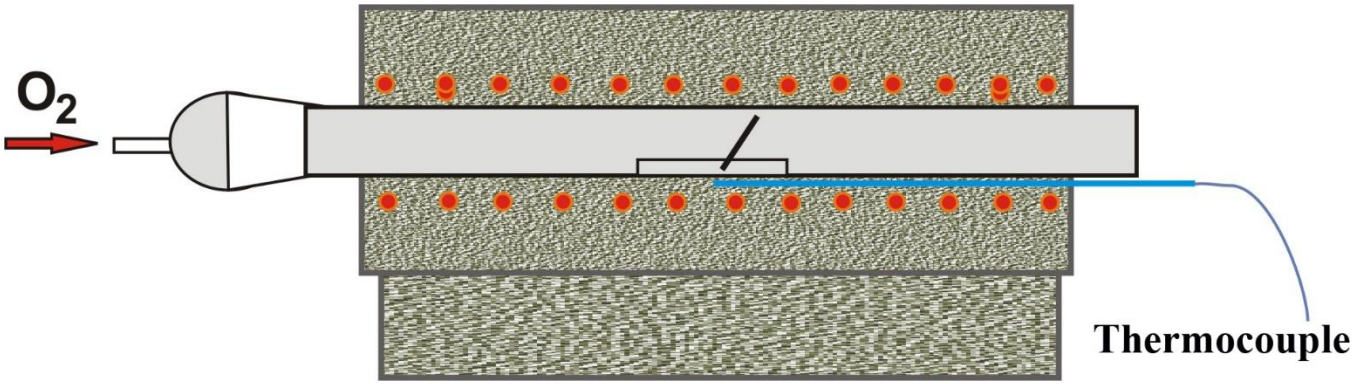

Furnace for oxidation of Pd films

Table 2. Regimes of Pd films oxidizing procedure.

Temperature *T*, K	670	770	870	1070	1120
Temperature, °C	400	500	600	800	850
Duration τ, min.	120				
Atmosphere	Dry oxygen				

New experimental results

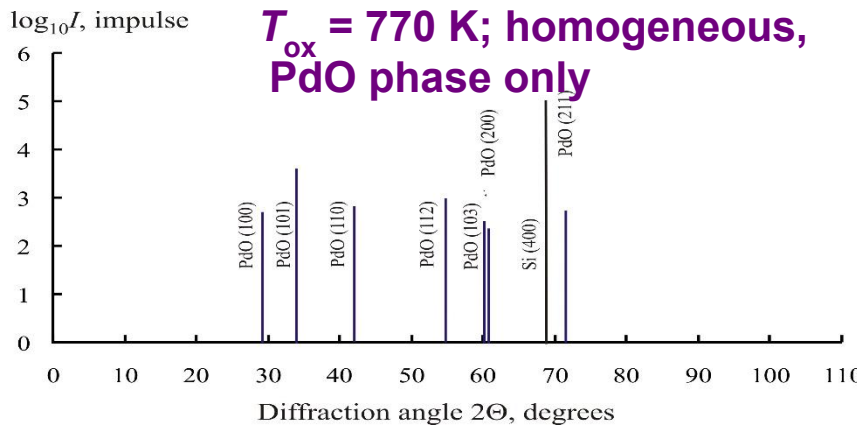

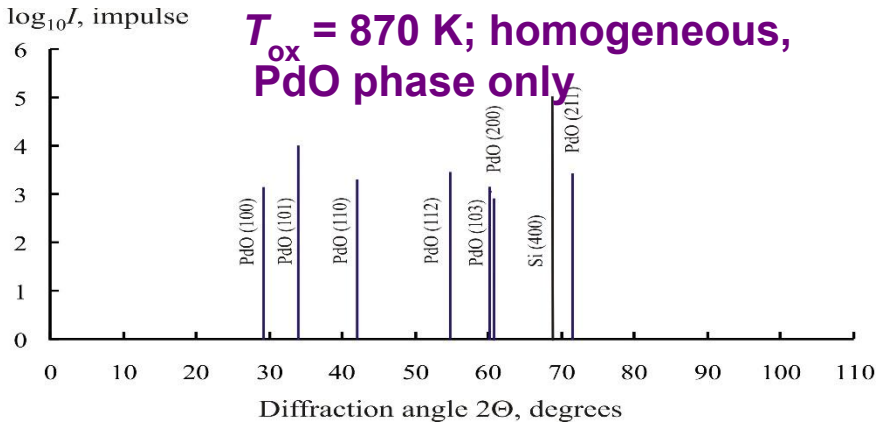

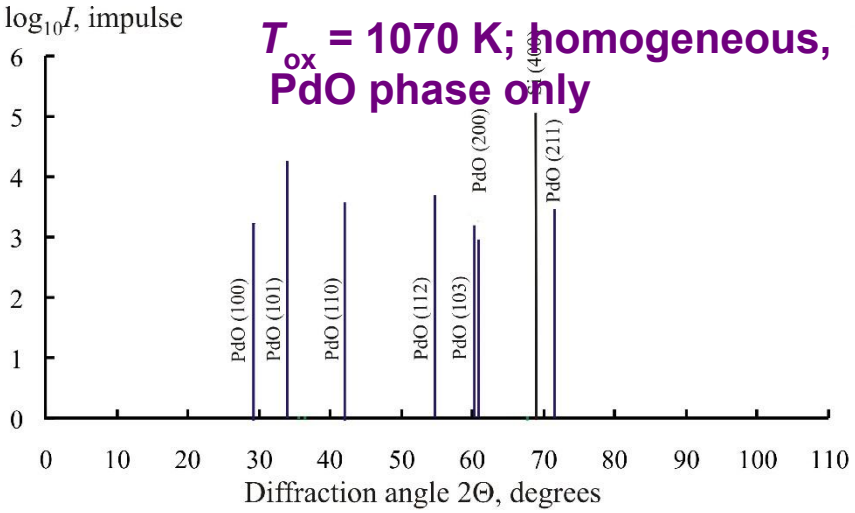

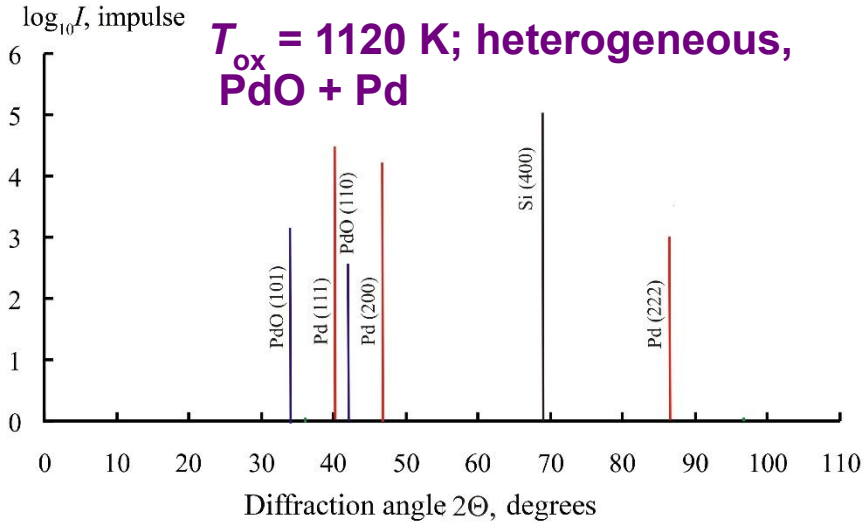

XRD patterns of PdO films on SiO_2/Si (100) substrates prepared by oxidation in dry oxygen.

New experimental results

EPMA EDS analysis of PdO films chemical composition

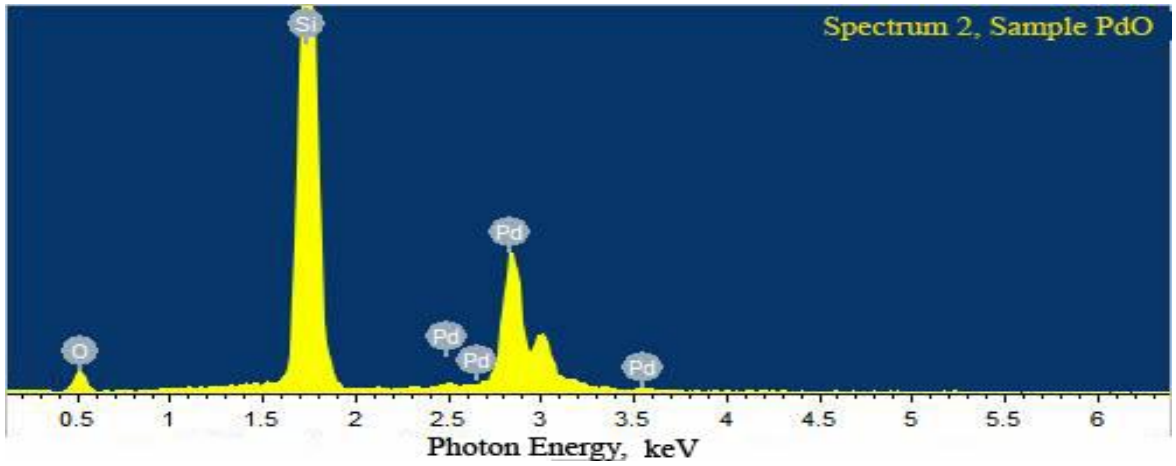

EDX spectrum of PdO film oxidized at *T* = 870 K, ambient air.

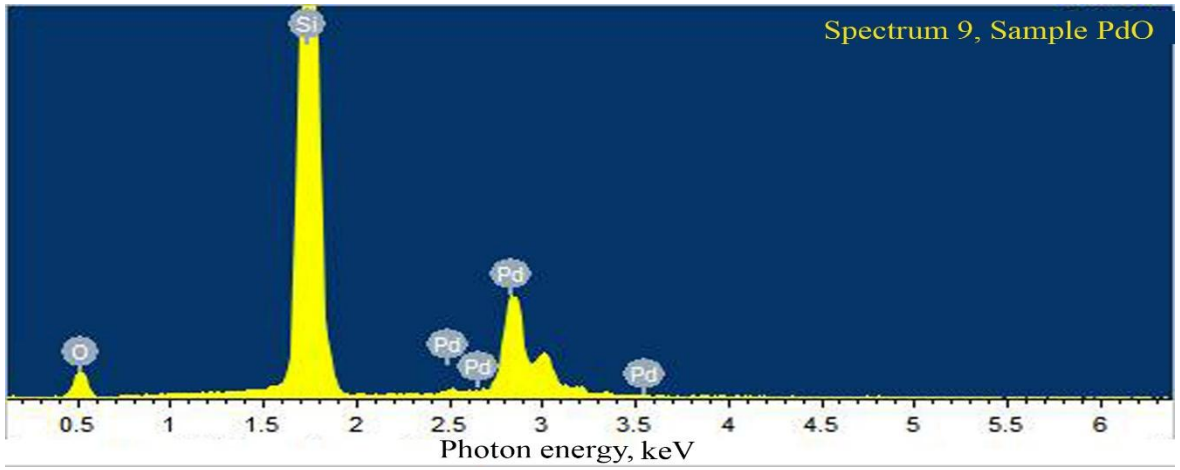

EDX spectrum of PdO film oxidized at *T* = 1070 K, dry oxygen.

New experimental results

EPMA EDS analysis of PdO films chemical composition

PdO films, thickness ~ 35 nm, oxidation in ambient air

Oxidation temperature T_{ox} = 870 K (600 °C)			
Element	X-ray spectrum line	Mass fraction ω, %	Mole fraction x, %
Palladium	L – line	36.93	11.985
Oxygen	K – line	11.24	24.275
Silicon	K – line	51.83	63.74
Total:		100 %	100 %
Composition:	n(Pd) : n(O) = 1 : 2.025		

Oxidation temperature T_{ox} = 1070 K (800 °C)			
Element	X-ray spectrum line	Mass fraction ω, %	Mole fraction x, %
Palladium	L – line	36.77	11.91
Oxygen	K – line	11.29	24.33
Silicon	K – line	51.94	63.76
Total:		100 %	100 %
Composition:	n(Pd) : n(O) = 1 : 2.043		

PdO films, thickness ~ 35 nm, oxidation in dry oxygen

Oxidation temperature T_{ox} = 870 K (600 °C)			
Element	X-ray spectrum line	Mass fraction ω, %	Mole fraction x, %
Palladium	L – line	36.55	11.81
Oxygen	K – line	11.37	24.44
Silicon	K – line	52.08	63.75
Total:		100 %	100 %
Composition:	n(Pd) : n(O) = 2.069		$PdO_{2,069 \pm 0,004}$

Oxidation temperature T_{ox} = 1070 K (800 °C)			
Element	X-ray spectrum line	Mass fraction ω, %	Mole fraction x, %
Palladium	L – line	36.26	11.67
Oxygen	K – line	11.5	24.61
Silicon	K – line	52.25	63.72
Total:		100 %	100 %
Composition:	n(Pd) : n(O) = 2,1088		$PdO_{2,109 \pm 0,004}$

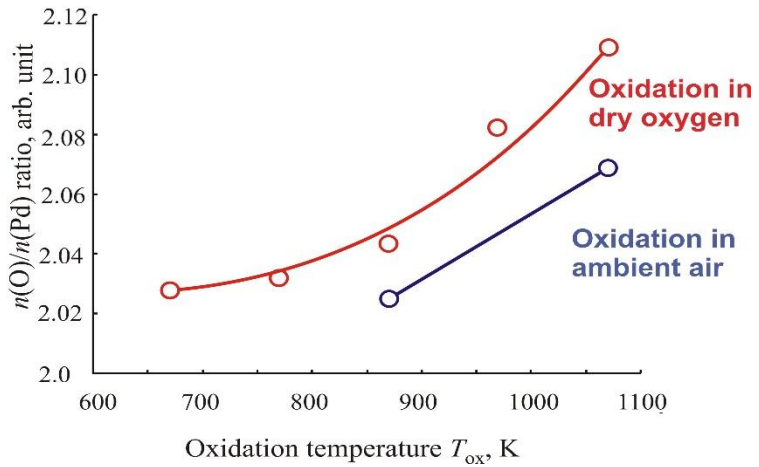

Dependence of n(O)/n(Pd) ratio upon oxidation temperature for PdO films oxidized in dry oxygen and ambient air.

New experimental results

XPS study of PdO films

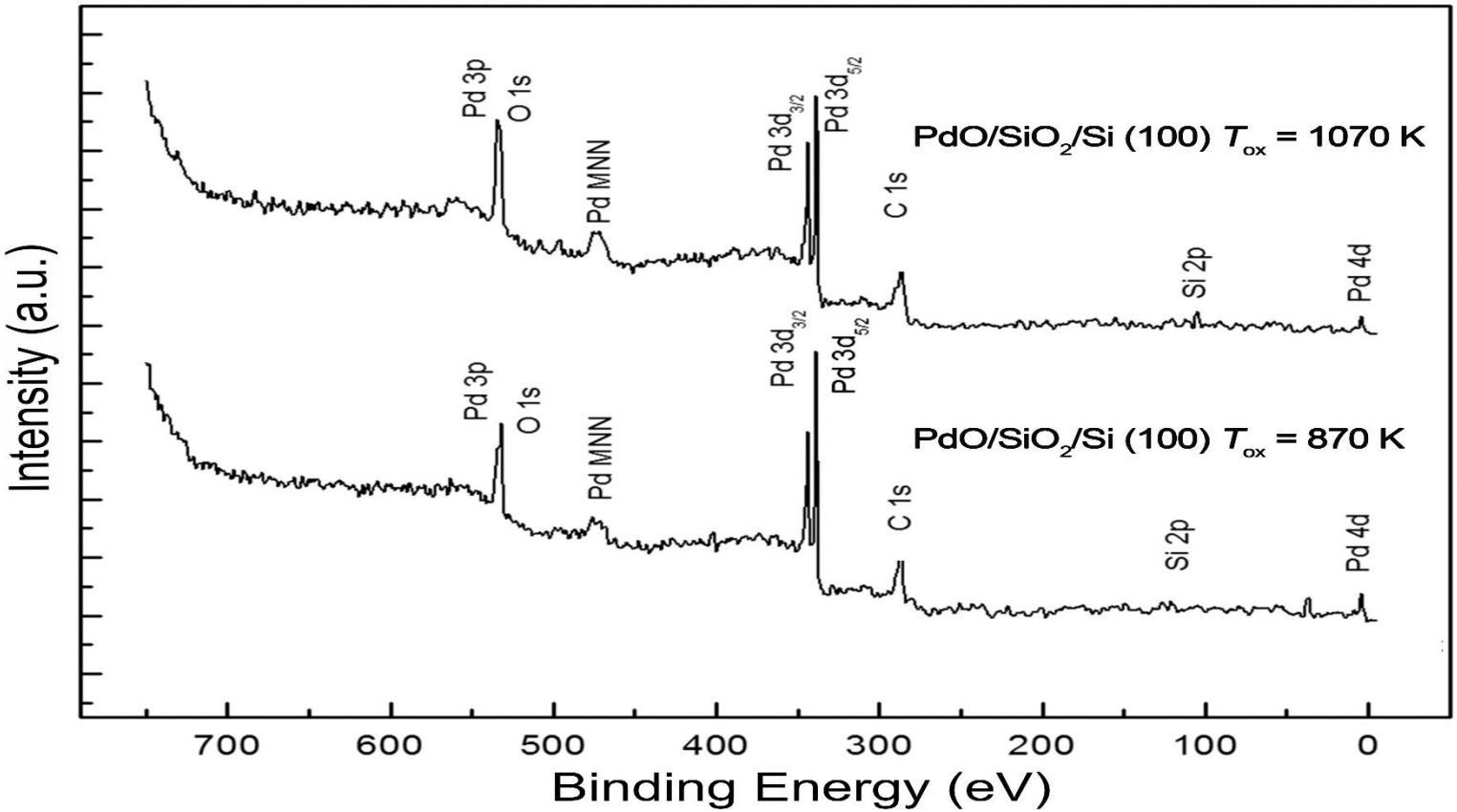

XPS surveys recorded for palladium oxide films obtained by oxidation at T_{ox} = 870 and 1070 K. Synchrotron quanta excitation energy was 800 eV.

New experimental results

XPS study of PdO films

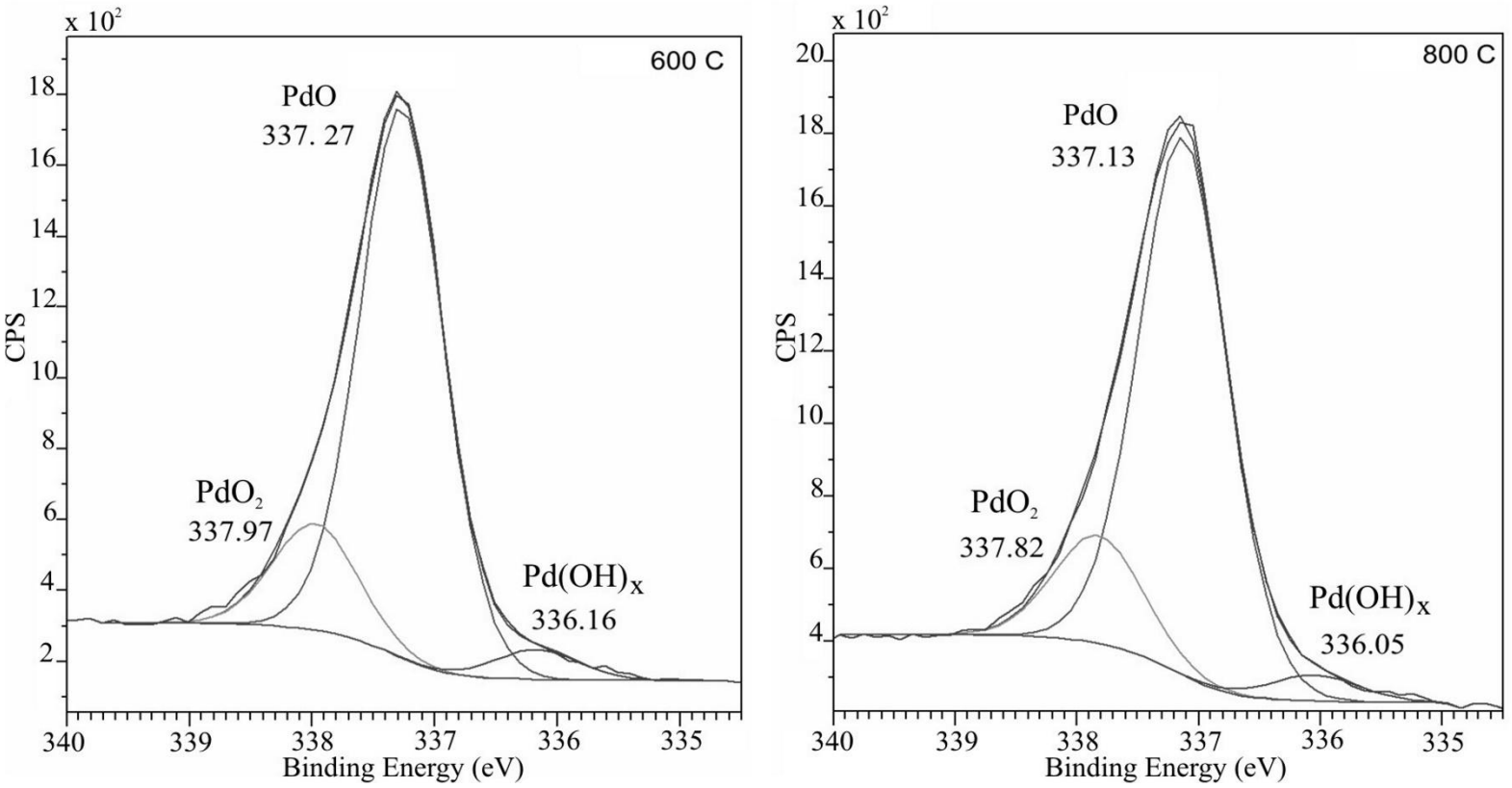

High resolution XPS Pd 3d5/2 core level for palladium oxide films prepared by oxidation at T_{ox} = 870 and 1070 K.

New experimental results

Taking into account all XRD reflexes palladium (II) oxide lattice constant a and c values have been calculated. Using the special software based on solution algorithm of quadric equation's system with two unobvious parameter the values of a and c lattice parameters of PdO tetragonal structure have been calculated. Nelson-Riley approximation for $2\Theta = 180$ degrees diffraction angle has been performed for the refinement and more precise determination of a and c lattice parameter values.

$$f(\theta) = 0.5 \times \left(\frac{\cos^2\theta}{\theta} + \frac{\cos^2\theta}{\sin\theta} \right)$$, where Θ is diffraction angle (radian).

Target value of lattice constant, for example a_0, have been calculated by linear approximation of $a = k \times f(\Theta) + a_0$ using the least-squares method.

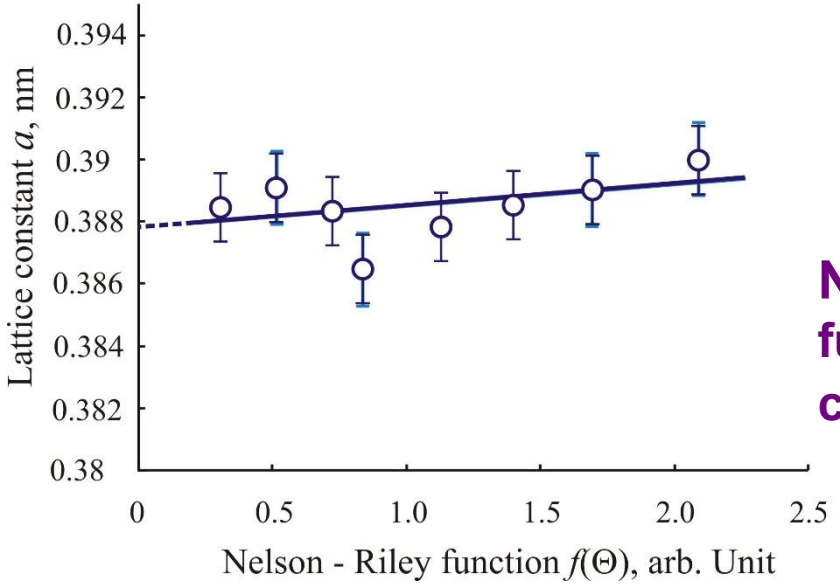

Nelson – Riley approximation function for calculation of lattice constant *a* of PdO films

New experimental results

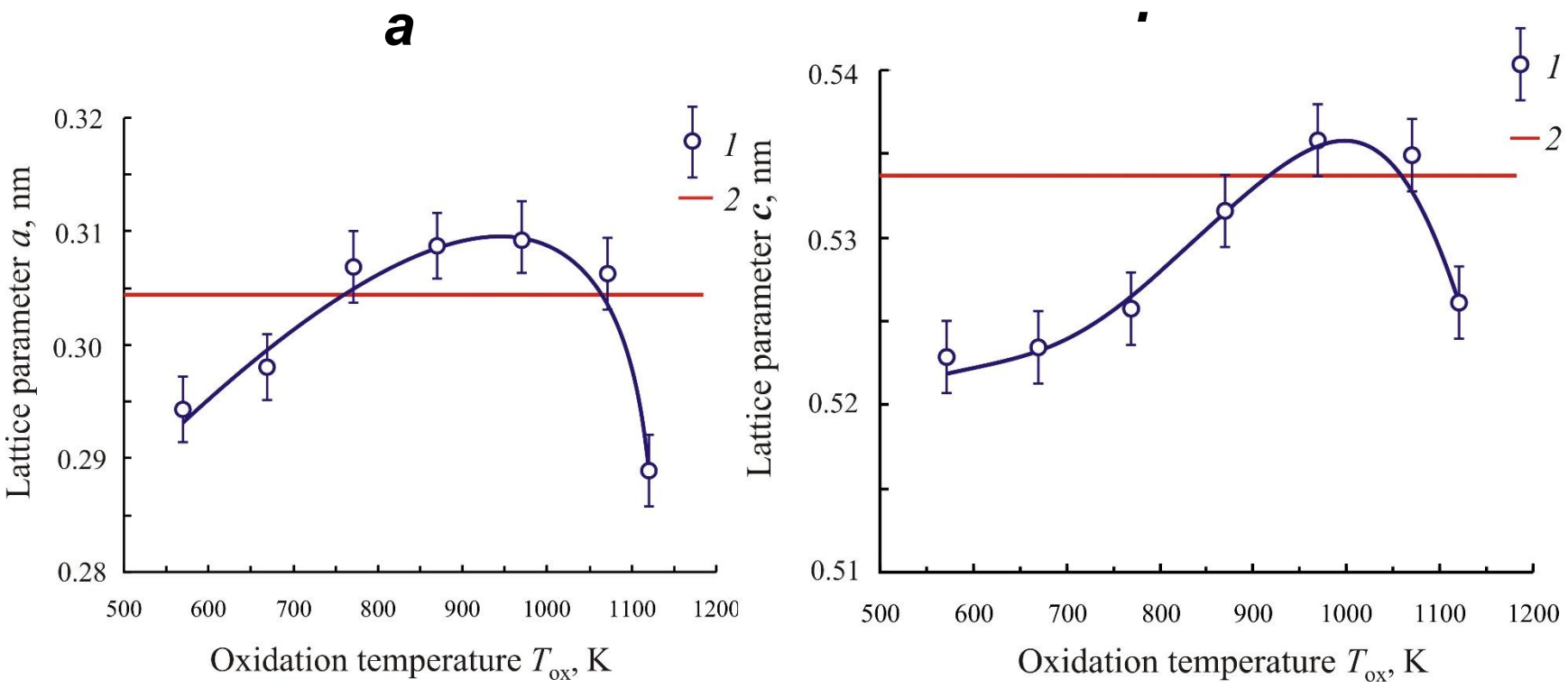

Dependence of PdO films lattice constant *a* (a) and c (b) upon temperature oxidation T_{ox} in dry oxygen:
***1* – our experimental results; *2* – ASTM etalon.**

New experimental results

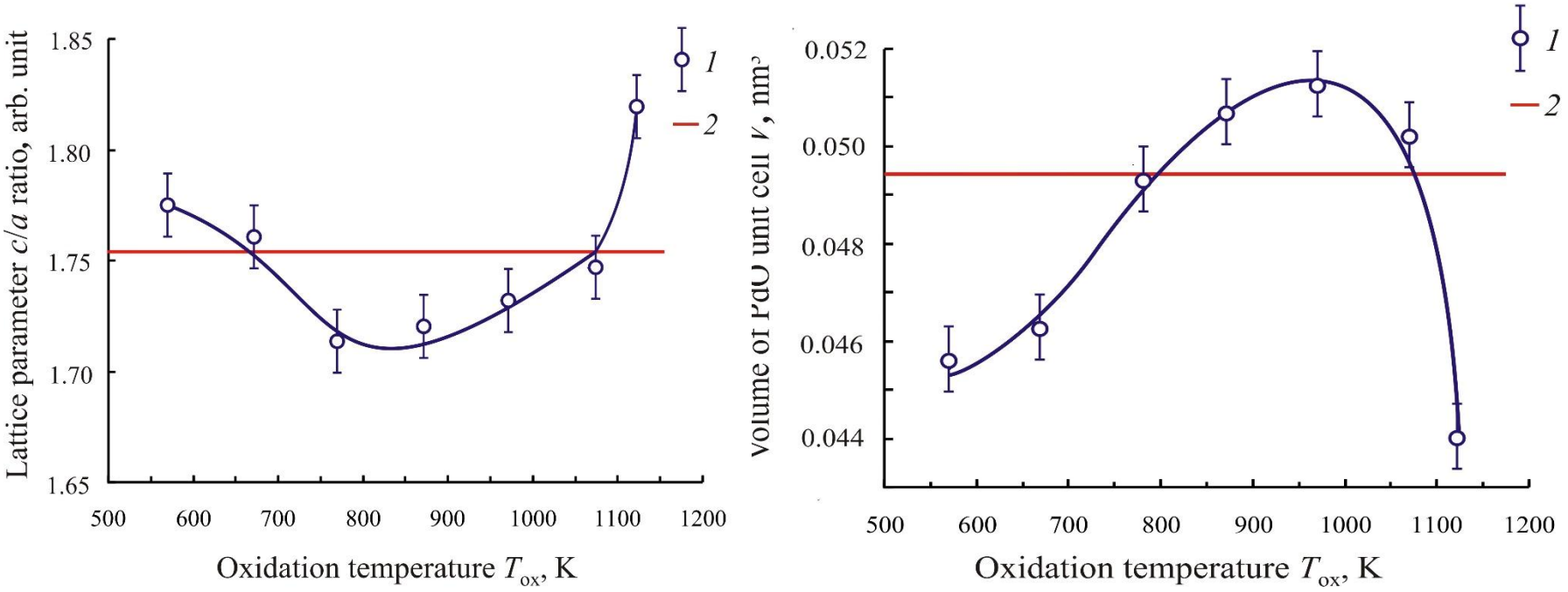

Dependence of PdO films of c/a lattice constant ratio (a) and unit cell volume V (b) upon temperature oxidation T_{ox} in dry oxygen: *1* – our experimental results; *2* – ASTM etalon.

Discussion of Experimental Results

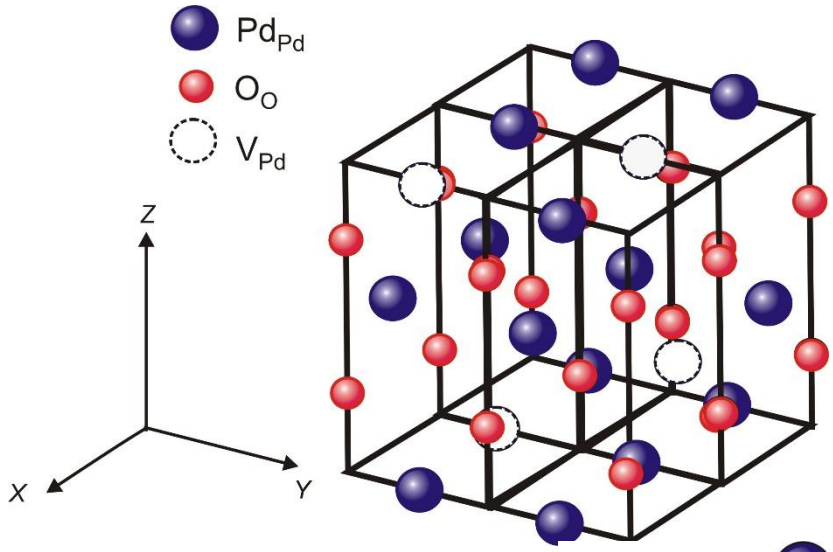

Crystal Structure of PdO with palladium vacancies V_{Pd} (4 unit cells).

2D projection of PdO Crystal Structure with palladium vacancies V_{Pd} on (001) plane (4 unit cells).

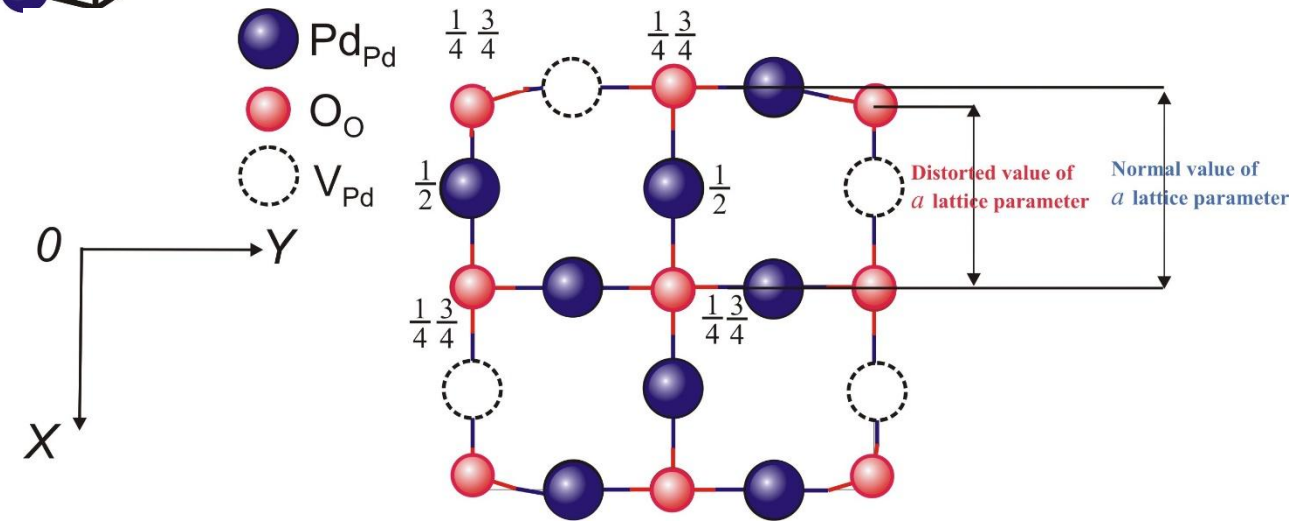

Discussion of Experimental Results

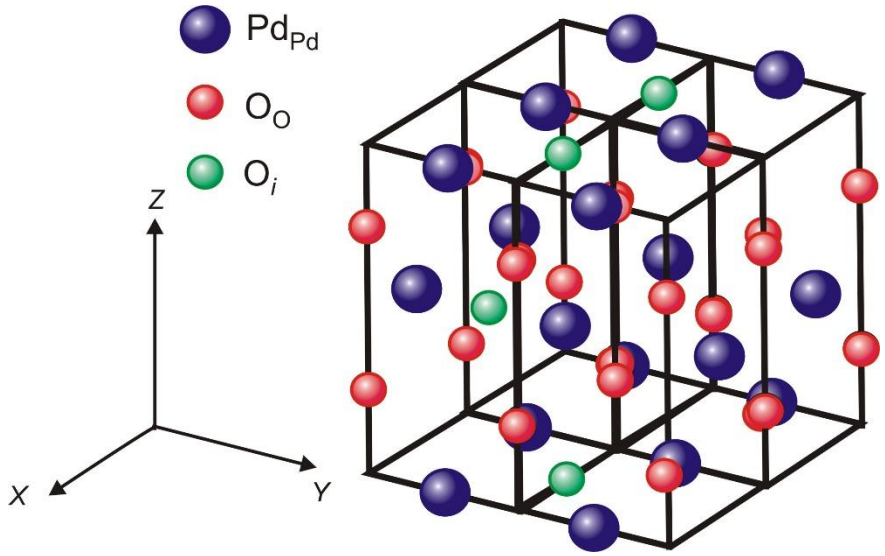

Crystal Structure of PdO with Oxygen atoms in interstitials O_i (4 unit cells).

2D projection of PdO Crystal Structure with oxygen atoms in interstitials O_i on (001) plane (4 unit cells).

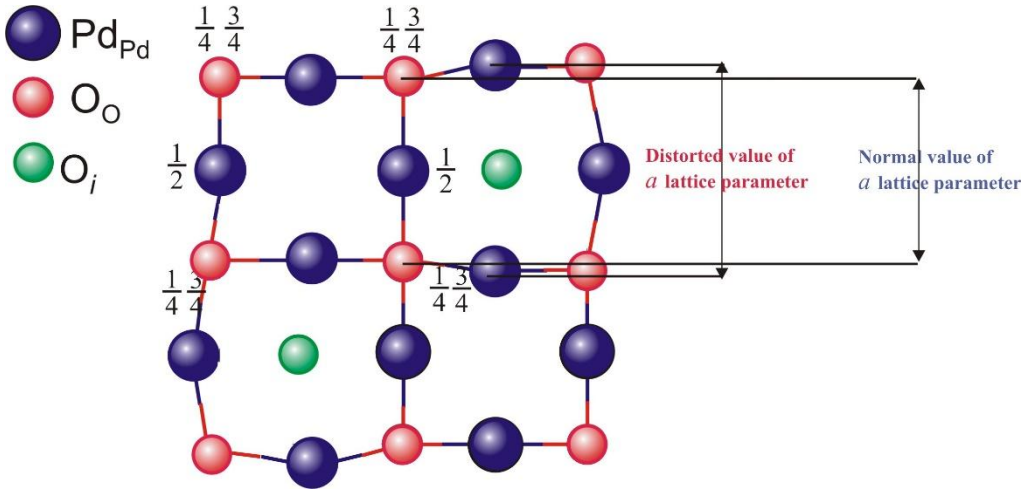

Summary and Conclusion

It is necessary to note that results obtained in this work are the part of PdO fundamentals from the Material Science point of view. Many of high temperature PdO properties have not studied yet because they did not use at application of this material as catalyst during organic synthesis.

1. By EPMA EDS results we have proved the hypothesis about PdO nonstoichiometry nature. We have proved that PdO exists with little excess of O atoms.
2. By EPMA EDS results it has been shown that the concentration of O atoms increases with increasing of the oxidation temperature.
3. By XPS study it has been found that PdO thin films contained trace amount of metastable palladium dioxide PdO_2.
4. By XRD study it has been established that dependence of PdO lattice constants upon the oxidation temperature had nonlinear character. From T = 570 to 970 K the values of these parameters increase and further decrease. At T = 1120 K PdO films decompose with Pd metal formation.
5. From the point of view of PdO nonstoichiometry the increase in lattice parameter and unit cell volume values can be interpreted as formation of excess O atoms in interstitials.

Future Study

The Hero at the Crossroad

The sensitivity of PdO based gas sensor can be improved by some ways:

1. **The optimization of morphology**

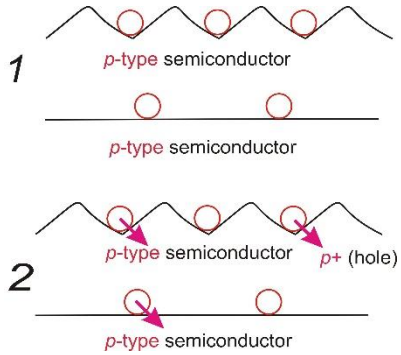

2. **Study of impact of nonstoichiometry degree upon the functional parameters.**

THANK YOU FOR YOUR ATTENTION!

If You have any questions or suggestion
You can find me:
Phone: +7 951 552 7564
+7 473 259 65 15
E-mail: samoylov@chem.vsu.ru

Future study

Why PdO films oxidized at *T* = 600 °C have been chosen for O_3 and NO_2 detecting?

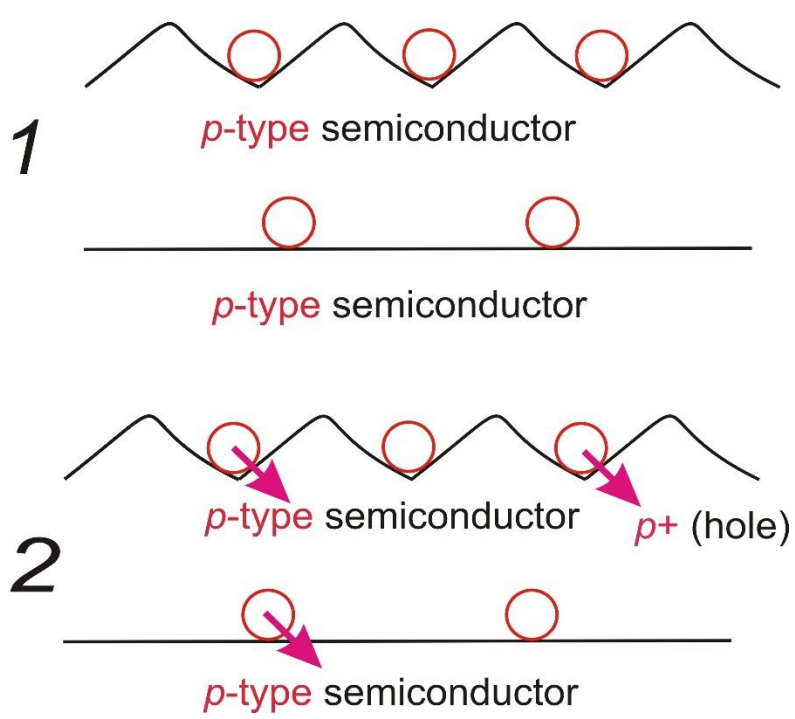

The decrease in semiconductor resistivity during gas detection process depends upon two factors:

1. the value of surface area – quantity of absorbed gas molecules;
2. the efficiency of interaction of gas molecules with semiconductor surface.

What factor does play the major role is not clear in this case.

Summary and Conclusion

Summary

Why PdO films oxidized at T = 600 °C have been chosen for O_3 and NO_2 detecting?

Table 7. The values of critical parameters of PdO films for oxidizing gas sensitivity.

Film / **Property**	Oxidizing at T = 300 °C	Oxidizing at T = 500 °C	Oxidizing at T = 600 °C	Oxidizing at T = 800 °C
Phase homogeneity	**No**	**Yes**	**Yes**	?????
Energy band gap ΔEg, eV	2.15	2.18	2.25	2.3
Surface area	Maximum	Middle range	Middle range	Maximum

Summary

Table 8. The values of maximum permissible concentration (critical concentration) averaged over one hour of ozone and nitrogen dioxide in industrialized countries.

Country / Gas	USA	UK	Japan	EC
Ozone	70 – 75 ppb	200 ppb	100 ppb	105 ppb
Nitrogen dioxide	100 ppb	100 ppb	100 ppb	100 ppb

Conclusion

At fabrication of gas sensors usage of $PdO_{1\pm x}$ thin films has ***some advantages*** in comparison with other materials.

Firstly, $PdO_{1\pm x}$ films have shown high values of sensor response, signal stability, and reproducibility of sensor response.

Secondly, the synthesis procedure of binary films $PdO_{1\pm x}$ is rather simple and is compatible with planar processes of a microelectronic industry also.

Work for Future

Because we started PdO investigation in September, 2015, today we have questions more then answers. We believe that nano crystal palladium oxide (films or ceramics) have perspectives to be one of the main materials for gas detection, at least, for detection gases with oxidizing properties.

Acknowledgements

Authors are thankful to the Russian Scientific Foundation (RSF) for financial support of this activity,
project no. 14-13-01470.